Classification of the geographical origin of Pinot noir wines from southwestern Switzerland using isotopes, volatile organic compounds, and chemometrics

Jorge Enrique Spangenberg [a], [1], *, Julien Baumann [a], Vivian Zufferey [b], [2]

[a] Institute of Earth Surface Dynamics (IDYST), University of Lausanne, Geopolis Building, 1015 Lausanne, Switzerland
[b] Research Center of Viticulture, Agroscope, 1009, Pully, Switzerland

ARTICLE INFO

ABSTRACT

This study examined the potential of carbon and nitrogen isotopes of wine solid residues with semi-quantitative amounts of volatile organic compounds to characterize Pinot noir wines from different regions in southwestern Switzerland. Significant differences in the ^{13}C/^{12}C (−30.6 to −26.4 mUr), ^{15}N/^{14}N (0.6–6.7 mUr), C/N (25–102), and contents of 38 volatiles exist between the wines. Principal component analysis identified three distinct clusters of wine regions: Valais, southern Vaud–Geneva, and Three Lakes. These clusters corresponded to a gradient in altitude, precipitation, temperature, and air humidity. The wine samples were satisfactorily classified according to their geographical origin using linear discriminant analysis on isotopic and molar ratios (84.8 % accurate prediction), selected volatile compounds (90.9 % accurate prediction), and the combination of both (95.5 % accurate prediction). Soil factors and aging in oak barrels did not affect the ability to classify wines based on the isotopic ratios and semi-quantified volatile compounds.

1. Introduction

Global climate change, plant water stress at the vine-region scale, and wine varietal suitability are major challenges for sustainable wine production (Santos et al., 2020; van Leeuwen et al., 2024). These factors can impact wine quantity and quality, resulting in substantial economic losses for vine growers, winemakers, and sellers. Therefore, consumers have become increasingly concerned with wine authenticity and potential health risks (Ubeda, Hornedo-Ortega, Cerezo, Garcia-Parrilla, & Troncoso, 2020). The development of new methods for tracing the geographical origins of wines has become an important issue worldwide, especially for wines with registered designations of origin (AOC, *Appellation d'Origine Contrôlée*). *Vitis vinifera* L. Pinot noir is an internationally appreciated wine produced in several European and New World countries and China. This temperate climate varietal is the most widely planted crop in Switzerland (https://www.blw.admin.ch/fr/statistiques-arboricoles-et-viticoles). The sensorial differences in Pinot noir wines due to their different geographical origins, pedoclimatic conditions (i.e., water availability), vintages, and aging history can be assessed via volatile organic compound (VOC) profiling (Cantu et al.,

2021; Fang & Qian, 2006; Herrero et al., 2016; Longo, Carew, Sawyer, Kemp, & Kerslake, 2021). The VOC profiles may be affected by various factors, such as vineyard topography, soil type, grape genotype, planting density, rootstock, vine age, vine vigor, and different stages of wine production, such as maceration/fermentation, post-maceration, aging in oak barrels, and storage in glass bottles (Ayestarán et al., 2019; Casassa, Huff, & Steele, 2019). In particular, water-stressed vines yield more complex and structured wines (Zufferey et al., 2017). Grapes from Pinot noir vines grown under moderate to high water stress give wines with more abundant alcohols, acetic acid, and phenols (Spangenberg, Vogiatzaki, & Zufferey, 2017). Several studies have proven the potential of stable isotope ratios of hydrogen, oxygen, and carbon (^{2}H/^{1}H, ^{18}O/^{16}O, ^{13}C/^{12}C, respectively, expressed as δ^{2}H, δ^{18}O, and δ^{13}C) to verify the geographical origins of wines. They used δ^{2}H and δ^{18}O values of wine water (Calderone & Guillou, 2008) combined with δ^{13}C and δ^{2}H of ethanol (Camin et al., 2015; Raco, Dotsika, Poutoukis, Battaglini, & Chantzi, 2015). The δ^{13}C values of berry sugars (δ^{13}C$_{sugars}$) increase in vines under water stress because the photosynthetic CO_2 fixation becomes limited due to stomatal closure, causing ^{13}C enrichment in the photosynthates. We showed that the linear relationship between the

---

* Corresponding author at: Av. des Cerisiers 61, 1009 Pully, Switzerland.
  E-mail address: Jorge.Spangenberg@unil.ch (J.E. Spangenberg).
[1] ORCID: 0000–0001–8636-6414.
[2] ORCID: 0000–0002–4686-5689.

Note: Low-resolution images were used to create this PDF. The original images will be used in the final composition.

$\delta^{13}C_{sugars}$ values and predawn leaf water potential (i.e., a measure of the plant water status) were preserved in the $^{13}C/^{12}C$ ratios of wine ethanol, whole wine, volatile compounds, and wine solid residues (Spangenberg et al., 2017; Spangenberg & Zufferey, 2019).

Few studies have used the isotope ratios of nitrogen ($^{15}N/^{14}N$ expressed as $\delta^{15}N$) of grape juice or wine samples. A ^{15}N labeling approach revealed that 90 % of the organic nitrogen content in grapes originated from sources other than fertilizers, including soil nitrogen or plant reserves (Verdenal et al., 2015). These findings suggested that the $\delta^{15}N$ values of off-vine grapes, grape juice, and wine can indicate their geographical origin. Another study examined the $^{15}N/^{14}N$ ratios along a soil-grape-wine system in northeastern Italy (Paolini et al., 2016); in particular, these authors found that fermentation did not affect the $\delta^{15}N$ values of grape must. Previous studies by our group demonstrated that the C/N molar ratios, $^{13}C/^{12}C$ and $^{15}N/^{14}N$ ratios of the wine solid residues (C/N$_{WSR}$, $\delta^{13}C_{WSR}$, and $\delta^{15}N_{WSR}$) for different varietals were highly correlated with the plant water status (Spangenberg et al., 2017; Spangenberg & Zufferey, 2018).

There are currently no studies investigating the applicability of the novel approach that involves analyzing carbon and nitrogen isotopes and molar ratios in wine solid residues for the geographical traceability of wines. The first hypothesis proposed in this study is that carbon and nitrogen isotopes and volatiles in wines are associated with climatic conditions, as we have shown for soil water availability. Therefore, these parameters can effectively distinguish between wines from different geographical origins. These analyses, which include $\delta^{13}C_{WSR}$, $\delta^{15}N_{WSR}$, and C/N ratios, can be combined with VOC profiling. Additionally, it is known that soil characteristics such as stoniness and carbonate content can affect the composition and quality of grapes and wine (Amorós et al., 2018). The potential compositional changes induced by soil parameters and oak aging may not significantly change the discrimination potential of the proposed analytical approach, leading to two further hypotheses to be tested.

Moreover, analyses of isotopes in solid residues and VOCs of commercial wines from Switzerland are still lacking. Therefore, this study aimed to investigate the above-mentioned hypotheses and address the existing research gaps. The objectives were achieved by comparing the $\delta^{13}C_{WSR}$, $\delta^{15}N_{WSR}$, C/N, and VOC concentrations in Pinot noir wine samples from terroirs in southwestern Switzerland.

2. Materials and methods

2.1. Chemicals

Dichloromethane and anhydrous sodium sulfate were purchased from Merck (Dietikon, Switzerland). The solvent was glass distilled shortly before use. A C_8–C_{20} n-alkane standard solution and the following standards for the identification of volatile compounds with a purity > 98 % were purchased from Merck and Sigma Aldrich (Buchs, Switzerland): 2-methylpropan-1-ol, butan-1-ol, 3-methylbutan-1-ol, hexan-1-ol, 4-methyl-pentan-2-ol, octan-2-ol, nonan-4-ol, ethyl(S)-2-hydroxypropanoate, phenyl acetate, acetic acid, butanoic acid, hexanoic acids, and octanoic acid. The chemicals used for packing the reactors of the elemental analyzer were purchased from Säntis Analytical (Teufen, Switzerland). Helium, nitrogen, and synthetic air (99.999 % purity) were obtained from Air Liquide/Carbagas (Lausanne, Switzerland).

2.2. Swiss Pinot noir regions and samples

Swiss wine production is spread across six wine regions: Valais, Vaud, German-speaking Switzerland, Geneva, Ticino, and Three Lakes. The wine regions from southwestern Switzerland are in the predominantly French-speaking cantons of Valais, Vaud, Geneva, Fribourg, Neuchâtel, and Bern (Fig. 1). The canton of Valais is traditionally di-

vided into upper, central, and lower Valais; the German–French linguistic border of the canton is located between the first two subregions (Fig. 1). The Three Lakes region includes the wine-growing areas on the banks of Biel, Neuchâtel, and Murten Lakes in the cantons of Fribourg, Neuchâtel, Bern, and the northern part of the canton of Vaud (Fig. 1). Sixty-seven Pinot noir wines from 2013 vintage were made available for this study after the 2015 "Mondial des Pinots" competition (Sierre, Valais, Switzerland, https://www.vinea.ch/mondial-des-pinots/). The wines originated from 30 wine-growing areas, including different AOC designations (Fig. 1).

The information on the sites from which the wine samples were obtained is summarized in Supplementary Table S1. According to the geographical location of the growing and production site, the samples were from seven regions: Upper Valais (UVS, sites 1 and 2), Central Valais (CVS, sites 3–8), Lower Valais (LVS, sites 9–11), southern Vaud (SVD, sites 12–18), Geneva (GE, sites 19–21), Three Lakes (TL, sites 22–29), and Thurgau (TG, site 30) (Fig. 1). The sample from the TG region provided the first data for a Swiss-German wine. Details on the 67 wines, including their growing sites, AOCs, and whether they were aged in oak barrels, are given in Table S2. Among the studied wines, 26 were aged in oak barrels, and 41 matured in steel tanks without contact with oak chips. The time spent in oak barrels was not written on the bottle label. In the studied regions, it generally ranged from three to six months. Swiss AOC wines can be blended with up to 10 % v/v of another wine (Swiss Federal Council, RS 817.022.110, Art. 8). We suppose that the chemical changes induced by this practice will not affect the overall discrimination potential of the proposed approach. Finally, two bottles of each wine were brought to the University of Lausanne in December 2015 and stored at 4 °C until analysis in February–June 2016.

2.2.1. Bedrock and soil types in the wine-producing regions

The wine-growing sites in Valais (UVS, CVS, and LVS) and the sites 12 and 13 of SVD are within the Swiss Southwestern Alps (Fig. 1). The other sites in SVD, GE, TL, and TG are in the Swiss Plateau, which is a lowland stretching from Lake Geneva to Lake Constance on the German border (Fig. 1). The bedrock lithologies, soil stoniness and carbonate occurrence for each site are presented in Table S1. The wine regions in Valais are mainly on Alpine Nappes, which consist primarily of sedimentary rocks (limestones and marls) and locally igneous and metamorphic rocks (granites, gneisses). The vineyards in the Swiss Plateau are on marine and freshwater molasse rocks consisting of eroded material (rock fragments, sand, silt, clay, sandstones, and marl) from the Jura Mountains and the Alps. The great mineralogical diversity of the bedrock lithology is reflected in the different textures and stoniness (i.e., not stony, stony, very stony, and extremely stony) and the wide variety and abundance of minerals in the vineyard soils. Based on the occurrenc of carbonate minerals, the sites were classified as "highly calcareous", "moderately calcareous", or "noncalcareous" (Table S1). Highly calcareous soils contain primarily carbonate minerals; moderately calcareous soils contain debris of carbonate-silicate shist and calcareous moraine; and noncalcareous soils contain marls, clays, silts, and sands.

2.2.2. Climate and weather in the wine-producing regions

The Atlantic Ocean influences the temperate oceanic climate of the Swiss Plateau (Cfb; Beck et al., 2023), which has no dry season and a warm summer. The Alps act as a climatic barrier between north and south and create complex microclimates in the inner-alpine valleys, which contain many vineyards (Fig. 1). Valais has the driest and most continental cooler climate (Dfb). For each site, we used the April–September 2013 average of mean daily temperature (ASMT), total precipitation (ASTP), mean air relative humidity (ASMRH), and mean global radiation (ASMGR) obtained from the nearest meteorological stations (https://www.agrometeo.ch/meteorologie). The April–September period corresponded to the vine vegetative cycle (i.e.,
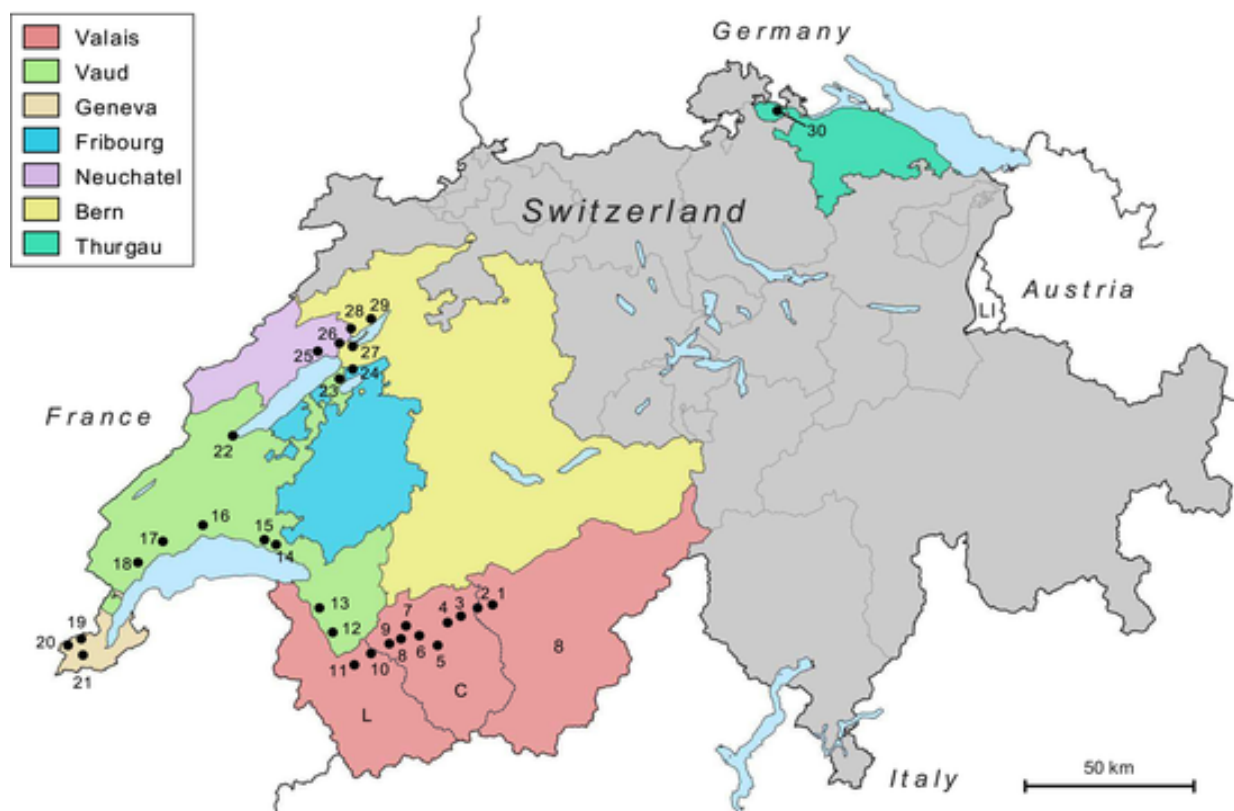
Fig. 1. Regions in Switzerland where the Pinot noir wine samples originated.
The sites listed from east to west and south to north include: 1–2: Upper Valais, 3–8: Central Valais, 10–11: Lower Valais, 12–18: Southern Vaud, 19–21: Geneva, 22–29: Three Lakes, 30: Thurgau.

most vine metabolisms were active). We calculated the bioclimatic indices, also known as agroclimatic indices, using the equations of Tonietto and Carbonneau (2004) for each wine-growing site. The drought index (DI) reflects the average vine water balance in September, while the cool night index (CI) indicates the average minimum temperature during the final maturation period. The heliothermal index (HI) is derived from the cumulative monthly air temperatures from April to September, adjusted with a coefficient based on day length, which varies according to the site latitude. The HI values identify areas suitable for viticulture (Tonietto & Carbonneau, 2004).

2.3. Separation of wine solid residue

The WSRs were obtained by freeze-drying subsamples of the wines following the procedure described in Spangenberg and Zufferey (2018). First, a 25 mL aliquot of wine was transferred from each bottle to a 50 mL wide-necked low-density polyethylene bottle with a screw cap (VWR International AG, Dietikon, Switzerland). The samples were frozen at −20 °C for two days before being freeze-dried using a Lyovac GT2 freeze-dryer (SRK Systemtechnik GmbH, Goddelau, Germany) for 48 h. The 50 mL bottle containing the WSR, which appears as a dense colloidal gel material, was closed and stored at −20 °C. The freeze-drying process was repeated using aliquots from a different bottle.

2.4. Carbon and nitrogen isotope analysis of WSRs

The $\delta^{13}C$ and $\delta^{15}N$ values of the WSRs were determined via elemental analysis and isotope ratio mass spectrometry (EA/IRMS) using separate combustions and sample aliquots of different weight sizes (Spangenberg & Zufferey, 2018, 2023). Aliquots of 50–250 µg and

4000–12000 µg WSR samples were weighed in tin capsules for $\delta^{13}C$ and $\delta^{15}N$ analysis. The EA/IRMS system consisted of an elemental analyzer (Carlo Erba 1108, Fisons Instruments, Milan, Italy) connected to an isotope ratio mass spectrometer via a split interface (Delta V Plus and Con-Flo III, both from Thermo Fisher Scientific, Bremen, Germany). The isotopic compositions were reported in delta (δ) notation and corresponded to the relative deviations of the molar ratio (R) of the heavy (^hE, ^{13}C or ^{15}N) to light (^lE, ^{12}C or ^{14}N) isotopes in the samples from those in the international standards:

$$\delta^i E_{sample} = \frac{R(^hE/^lE)_{sample}}{R(^hE/^lE)_{standard}} - 1$$

For the $\delta^{13}C$ values, Vienna Pee Dee Belemnite limestone (VPDB) was the standard; for the $\delta^{15}N$ values, Air-N_2 (molecular nitrogen in air) was the standard. According to the guidelines and recommendations of the International Union of Pure and Applied Chemistry (IUPAC), the International System of Units (SI) unit for delta values is the urey (symbolized Ur). The δ-value from the above equation was multiplied by 1000, and the unit is milliurey (mUr). The $\delta^{13}C$ and $\delta^{15}N$ values were normalized using a three-point calibration. The following international reference materials (RMs): USGS64 ($\delta^{13}C_{VPDB}$ = −40.81 mUr and $\delta^{15}N_{Air-N2}$ = +1.76 mUr), USGS65 ($\delta^{13}C_{VPDB}$ = −20.29 mUr and $\delta^{15}N_{Air-N2}$ = +20.68 mUr), USG66 ($\delta^{13}C_{VPDB}$ = −0.67 mUr and $\delta^{15}N_{Air-N2}$ = +40.83 mUr), USGS-600 ($\delta^{15}N_{Air-N2}$ = +1.02 mUr), and USGS40 ($\delta^{15}N_{Air-N2}$ = −4.52 mUr) were used. The repeatability and intermediate precision of the $\delta^{13}C_{WSR}$ and $\delta^{15}N_{WSR}$ measurements were determined by the standard deviation of separately replicated analyses of RMs (n = 8) and were better than ±0.1 mUr. The total organic carbon and total nitrogen contents (wt% TOC and TN, respectively) were

determined from the sum of the major peak areas. The repeatability was better than 0.2 wt% for the C and N concentrations. The C/N molar ratios (C/N$_{WSR}$) were derived from the TOC and TN values. The results were an average of four to eight replicates.

2.5. Analysis of volatile organic compounds (VOCs)

The VOCs were extracted and analyzed using the procedures described in Spangenberg et al. (2017). The extraction was performed using a method modified from Ferreira, López, Escudero, and Cacho (1998). The original protocol, suitable for wines relatively rich in VOCs, was scaled up for high-volume extraction of Swiss Pinot noir wines. Samples were homogenized by shaking before the analysis. In brief, 50 mL of wine was transferred to a 100 mL amber glass bottle and 400 μL of an internal standard mixture of 4-methylpentan-2-ol (final concentration of 28.484 mg/L), octan-2-ol (22.157 mg/L), and nonan-4-ol (22.736 mg/L) in dichloromethane (DCM) was added. Then, 10 mL of DCM was added, and the bottle was tightly closed and shaken for 30 min at a speed of 250 rpm on a rotating/rocking shaker (Fisher Scientific AG, Reinach, Switzerland). The mixture was then transferred to a 100 mL glass separatory funnel equipped with a Teflon® (PTFE) stopcock and stopper. After 2 h of separation, the DCM layer containing the VOCs was transferred to a 15 mL Pyrex glass tube with a Teflon-lined screw cap and centrifuged at 4000 rpm for 10 min (Eppendorf® 5702 centrifuge, Schänbuch, Switzerland). The organic phase was recovered, dried over anhydrous Na$_2$SO$_4$, transferred to a 2 mL vial with a Teflon-lined screw cap, concentrated under a stem of pure nitrogen to a final volume of 500 μL and then stored in the dark at −20 °C before analysis. The extraction was repeated two to three times.

The extracted VOCs were chemically characterized by gas chromatography/mass spectrometry (GC/MS) using an Agilent 6890 gas chromatograph (Agilent Technologies, Palo Alto, CA, USA) connected to an Agilent 5973 mass selective detector operating at 70 eV (source 230 °C and quadrupole 150 °C) in electron ionization mode, with a current emission of 1 mA, and full scan mode from *m/z* 10 to 500. An Agilent DB-WAXetr fused-silica column (60 m × 0.25 mm i.d., 0.50 μm film thickness) was used to separate the VOCs. The samples were injected splitless at 250 °C. After an initial period of holding the oven at 40 °C for 5 min, the oven was heated at 4 °C/min to 250 °C and held at that temperature for 16 min. A constant helium flow of 1.4 mL/min was used. The compounds were initially tentatively identified by comparing the unknown mass spectra with those in the NIST14 mass spectral library (National Institute of Standards and Technology, Gaithersburg, MD, USA) and using published elution orders and retention times. It was followed by matching the experimental linear retention index (LRI$_{exp}$) with retention indices from literature (RI$_{lit}$) obtained using polar columns (https://webbook.nist.gov/chemistry). The LRI$_{exp}$ values were calculated by the no-isothermal Kovats index equation (https://webbook.nist.gov/chemistry) using a mixture of C$_8$–C$_{20}$ *n*-alkanes analyzed under the same GC/MS conditions as those used for the wine samples. The range (minimum and maximum), average, and standard deviation of the published RI values for DB-Wax or equivalent polar columns and temperature programming conditions are given in Table S3. When possible, the assignment of the VOCs was further verified by comparing the retention times and MS fragmentation data with those of standards. The GC/MS analysis was performed in duplicate.

Gas chromatography/flame ionization detection (GC/FID) analyses of the volatile compounds were performed using an Agilent Technologies (Wilmington, DE, USA) 7890B GC system equipped with a 7693A automated injection system and a flame ionization detector (FID, Agilent 7890). The chromatographic conditions were similar to those used for the GC/MS, except for the helium flow rate: same DB-WAXetr column, splitless injector at 250 °C, initial oven temperature of 40 °C, hold for 5 min, increase to 250 °C at 4 °C/min, hold for 18 min, and helium as the carrier gas at a flow rate of 2.2 mL/min. The FID was operated at 280 °C, with a hydrogen flow rate of 30 mL/min, synthetic air flow of 400 mL/min, and a make-up nitrogen flow of 25 mL/min. The helium flow rate was optimized for the alignment of the GC/MS and GC/FID signals (retention times in Table S3). The GC/FID data and the internal standard octan-2-ol were used for semi-quantification. The quantity of volatile compounds was calculated by dividing the area of the peak of each compound by the area of the internal standard and multiplying this ratio by its concentration.

2.6. Statistical analysis

The complete dataset for the 67 wine samples included the following parameters: canton, Pinot noir wine region, wine-growing site, AOC, terroir, geographical coordinates, altitude, bedrock lithology, surficial formation, soil texture, agrometeorological measurements, bioclimatic indices, maturation in oak barrels or storage in stainless steel tank, $\delta^{13}C_{WSR}$, $\delta^{15}N_{WSR}$, C/N$_{WSR}$, semi-quantitative data for VOCs and VOC groups, including alcohols (Tal), esters (Tet), carboxylic acids (Tac), carbonyl compounds (Tcc), phenolic compounds (Tph), lactones (Tla), nitrogen compounds (Tni), and sulfur compounds (Tsu). Statistical analyses were performed using SPSS Statistics software for Mackintosh (Version 29.0.2.0; IBM, Armonk, NY, USA). Differences ($P < 0.05$) between the geographical sites of the wines were determined via descriptive analyses and mean comparisons via analysis of variance (ANOVA). The post hoc Tukey's honest significance test (HSD) and the less conservative Fischer's least significant test (LSD) were used. The HSD and LSD results were compared and used to constrain the geographical grouping of wines. Principal component analysis (PCA) of the Pearson correlation matrix with no rotation was used to elucidate associations between the variables (e.g., stable isotopes and VOC concentrations) and wine samples. PCA was used to identify the main sources of variation and enabled the reduction of dimensionality to a few new variables (principal components, PCs); PCs are linear combinations of the original variables. The PC scores were interpreted geometrically as the projection of the observations on the PCs, revealing relationships between wine samples. Linear discriminant analysis (LDA) was used to evaluate the classification of the groups via one-way ANOVA and PCA and to identify the variables that characterized the different wine groups or wine-growing sites. LDA is a supervised method that maximizes the between-class variance and minimizes the within-class variance. A stepwise LDA procedure was used to select the variables. The performance of the LDA model was evaluated in terms of the correct classification rate on the entire modeling set (recognition ability) and the leave-one-out cross-validation procedure (prediction ability). Two-way ANOVA with the general linear model (GLM) procedure was used to assess the importance of the geology (i.e., bedrock lithology) and soil conditions (carbonate content and texture) on the geographical grouping of wines according to the PCA and LDA results. Two-way ANOVA was used to investigate the potential relationship between the geographical classification of samples and the type of aging container. The software used for preparing the figures included DeltaGraph (V7.1.3, Red Rock Software Inc., UT, USA), Adobe Illustrator 2022 (V27.1.1, Adobe Systems Inc., CA, USA), and 2022 Microsoft PowerPoint (V16.69.1). The three-dimensional scatterplots were prepared with Excel macros (https://www.doka.ch/Excel3Dscatterplot.htm) and imported into PowerPoint.

3. Results and discussion

3.1. Geoclimatic parameters

The agrometeorological measurements and bioclimatic indices for each sampling site are given in Table S1. One-way ANOVA and multiple comparisons ($P < 0.05$) were performed on these data to reveal potential differences between wine regions. The results are listed in Table 1

Table 1
Geoclimatic parameters for the Pinot noir wine regions.

Region (N)	UVS (24)	CVS (12)	LVS (4)	SVD (10)	GE (3)	TL (13)	TG (1)
Latitude	46° 18′ 45″ N	46° 15′ 39″ N	46° 10′ 58″ N	46° 26′ 54″ N	46° 11′ 31″ N	46° 59′ 25″ N	47° 40′ 12″ N
Longitude	7° 34′ 39″ E	7° 26′ 24″ E	7° 12′ 38″ E	6° 38′ 22″ E	6° 01′ 17″ E	6° 0′ 21″ E	7° 26′ 11″ E
Altitude (masl)	692 ± 1^a	678 ± 20^a	562 ± 28^b	498 ± 16^c	443 ± 17^c	476 ± 5^c	460
Slope (%)	14.5 ± 1.1^a	14.2 ± 1.7^a	11.8 ± 1.6^{ab}	12.7 ± 1.6^{ab}	10.3 ± 0.9^b	14.1 ± 0.5^a	13.0
Climate type	Dfb	Dfb	Dfb	Cfb	Cfb	Cfb	Dfb
ASMT (°C)	16.0 ± 0.1^{ab}	16.3 ± 0.1^{ab}	16.5 ± 0.2^a	16.2 ± 0.16^{ab}	15.9 ± 0.3^b	15.4 ± 0.1^c	15.1
ASTP (mm)	310 ± 4^a	287 ± 11^a	355 ± 19^a	646 ± 33^b	667 ± 51^b	693 ± 32^b	554
ASMRH (%)	63.8 ± 0.0^a	63.9 ± 0.3^a	69.1 ± 2.2^b	75.2 ± 0.8^c	73.6 ± 1.4^c	76.4 ± 3.3^c	77.2
ASMGR (Wm^{-2})	198 ± 0.3^a	203.0 ± 1^a	214 ± 8^a	198 ± 3^a	204 ± 9^a	202 ± 4^a	193
DI (mm)	159 ± 3^a	125 ± 8^a	148 ± 45^a	364 ± 21^b	351 ± 14^b	374 ± 14^b	309
CI (°C)	11.29 ± 0.02^{ab}	11.48 ± 0.05^{ab}	10.33 ± 0.48^c	12.06 ± 0.30^a	10.98 ± 0.48^{bc}	11.51 ± 0.18^{ab}	11.5
HI	1973 ± 25^a	1792 ± 2^{bc}	1832 ± 10^b	1665 ± 34^{cd}	1652 ± 60^d	1543 ± 42^d	1776

UVS: Upper Valais, CVS: Central Valais; LVS: Lower Valais; SVD: Southern Vaud; GE: Geneva; TL: Three Lakes; TG: Thurgau. Number of sampling sites (shown in Fig. 1) in brackets. Geographical coordinates were obtained by averaging the values for the sites within a region. Cfb = Temperate without a dry season and warm summer; Dfb = Cold without a dry season and warm summer. Values are given as means ± standard errors of sampling sites (N) within the same region. Means with different lowercase letters in the same row are significantly ($P < 0.05$) different based on Tukey HSD test.

and presented as boxplots in Supplementary Fig. S1. The altitude of the wine regions decreased from 780 m above sea level (masl) in Upper Valais to 419 masl in Geneva, following the order UVS ≈ CVS > LVS > SVD ≈ TL ≈ TG ≈ GE. The mean April–September temperature was significantly lower in TL and TG than in the other regions. The lowest total precipitation and relative humidity were in the subregions of Valais. The ASTP values followed the order UVS ≈ CVS ≈ LVS < TG < SVD ≈ GE ≈ TL, and the ASMRH values UVS ≈ CVS < LVS < SVD ≈ GE ≈ TL ≈ TG. The mean global radiation was low in TG and high in LVS (statistically not significant). There were no significant differences in the mean global radiation between regions (Table 1). The average drought index values showed significant differences between groups of regions. The Valais subregions (UVS, CVS, LVS) had DI values in the 50–150 mm range, and the SVD, GE, and TL regions had DI > 150 mm, consistent for sub-humid and humid viticultural climates, respectively (Tonietto & Carbonneau, 2004). In all sites, the CI values were < 12 °C, indicating areas for viticulture with very cold nights. The LVS region has the lowest statistically significant value. The average heliothermal index values were within 1800–2000 for UVS, CVS, and LVS and 1500–1800 for SVD, GE, TL, and TG regions (Table 1). This trend indicates a shift in the climate of the wine regions from temperate to cool. As Pinot noir is a cool-climate variety, the HI values suggested that suitability for viticulture in 2013 varied among areas in the order UVS < CVS ≈ LVS < SVD ≈ GE ≈ TL (Table 1). The altitude, meteorological data, and bioclimatic indices suggested distinct groupings among the Valais subregions. For this reason, in the first instance, UVS, CVS, and LVS were considered a single group. Consequently, wine regions with different geoclimatic conditions were Valais, southern Vaud-Geneva, and Three Lakes.

3.2. Carbon and nitrogen isotope ratios of the wine solid residue

The WSRs of all the wine samples had $\delta^{13}C$ values between −30.6 and −26.4 mUr (mean ± 1 SD, −28.8 ± 0.9 Ur, N = 67) and $\delta^{15}N$ values between 0.6 and 6.7 mUr (3.7 ± 1.2 Ur), whereas the C/N molar ratios varied from 25 to 102 (45 ± 16) (Table 2). The broad range of 4.2 mUr values in the $\delta^{13}C_{WSR}$ values was similar to those reported for Pinot noir wines from the 2009–2014 irrigation experiments and the 2020–2021 soil management field trials in Leytron (canton of Valais) (Spangenberg et al., 2017; Spangenberg & Zufferey, 2023). The average $\delta^{13}C_{WSR}$ values decreased from UVS to TL and TG sites (Table 2). The UVS and CVS regions differed significantly ($P < 0.05$) from GE and TL. No significant differences were between LVS, SVD, GE, and TL. These trends were similar to those shown for altitude and temperature and opposite to precipitation and relative humidity (Tables 1 and 2). These

similarities indicated that the differences in the $\delta^{13}C_{WSR}$ values of Swiss Pinot noir wines were caused primarily by changes in soil water availability in the wine regions. The relationship between the $\delta^{13}C_{WSR}$ values and the $\delta^{13}C$ values of photosynthates (sugars) in grapes supports this deduction (Spangenberg et al., 2017). Carbon isotope discrimination during photosynthesis in C_3 (i.e., the Calvin-Benson cycle) plants is affected by environmental changes. For a given atmospheric CO_2 concentration, a soil water deficit reduces the stomatal conductance, photosynthetic activity, and ability for carbon isotope discrimination (Medrano, Escalona, Bota, Gulías, & Flexas, 2002). The organic compounds in the wine solid residues, obtained by freeze-drying wine aliquots, included the nonvolatile residual fermentable sugars (glucose, fructose, and sucrose), nonfermentable sugars (arabinose, xylose, ribose, and rhamnose), nitrogenous organic compounds, tartaric acid, and trace amounts of low-volatile organic compounds such as $C_{>5}$ esters, ketones, terpenes, C_{13} norisoprenoids, C_6 alcohols, phenolic compounds, and fatty acids (de Torres, Diaz-Maroto, Hermosin-Gutierrez, & Perez-Coello, 2010; Spangenberg et al., 2017). All of these organic compounds in the wine originated from the C-atoms of the photosynthates (glucose and fructose) through different metabolic processes in the vine, off-vine grape, and fermentation of grape juice. Therefore, the differences in the $\delta^{13}C_{WSR}$ values reflected the variation in stomatal conductance and water availability between the vine cultivars in the different wine regions. In addition to stomatal conductance (g_s), the photosynthetic yield and carbon isotope fractionation are affected by other physical and biochemical factors, including mesophilic conductance (g_m), photochemical efficiency, and (Rubisco) carboxylation activity and kinetics; these factors are driven by irradiance, temperature, and nitrogen availability (Evans & von Caemmerer, 2013). High temperature and irradiance increased g_m and the photochemical efficiency and lowered the carbon isotope discrimination; these factors added to the effect of low g_s caused by the soil water deficiency, which increased the $\delta^{13}C$ values. The effect of these processes was shown by the ~1.5 mUr higher $\delta^{13}C_{WSR}$ values of the wines from the upper and central Valais regions than those from Three Lakes sites, which had higher average precipitation, air humidity, and lower temperatures (Tables 1 and 2).

The $\delta^{15}N_{WSR}$ values were higher in wines from UVS, CVS, LVS, and SVD than those from GE, TL, and TG regions (Table 2). The wines from Valais had the lowest C/N values, wines from Geneva the highest, and intermediate values had wines from regions SVD and TL (Table 2). These results revealed differences in the concentrations and sources (with distinct $\delta^{15}N$ values) of soil nitrogen available to vines in the different regions. By using identical cultivation techniques in vineyards with similar bioclimatic indices (e.g., DI, CI, HI values) in the canton of Vaud, Reynard, Zufferey, Nicol, and Murisier (2011) demonstrated that

Table 2

Pinot noir wines isotopic ratios (mUr) and semi-quantitative concentrations of volatile organic compounds (mg/L equivalent to octan-2-ol).

Variable	Code	Peak nr	LRI$_{exp}$	ID method	UVS (24)	CVS (12)	LVS (4)	SVD (10)	GE (3)	TL (13)	TG (1)
$\delta^{13}C_{WSR}$					-28.16 ± 0.10^a	-28.44 ± 0.16^a	-28.94 ± 0.21^{abc}	-29.21 ± 0.31^{bc}	-29.78 ± 0.53^c	-29.67 ± 0.12^c	-29.66
$\delta^{15}N_{WSR}$					4.29 ± 0.17^a	4.18 ± 0.11^a	4.53 ± 0.15^a	3.84 ± 0.36^a	1.77 ± 0.50^b	2.22 ± 0.25^b	1.93
C/N$_{WSR}$					37.9 ± 1.7^{ab}	40.8 ± 1.8^{ab}	28.3 ± 1.3^a	53.4 ± 6.2^b	91.6 ± 8.1^d	50.7 ± 2.4^b	27.3
VOC common name [IUPAC name]											
Alcohols											
Isobutyl alcohol [2-methylpropan-1-ol]	al1	1	1106	A, B, C	15.4 ± 0.4^a	15.1 ± 1.0^a	16.8 ± 1.2^{ab}	19.6 ± 1.7^{ab}	19.3 ± 2.0^{ab}	22.8 ± 1.7^b	21.0
1-butanol [butan-1-ol]	al2	3	1151	A, B, C	0.41 ± 0.01^{ab}	0.44 ± 0.02^a	0.44 ± 0.05^a	0.35 ± 0.02^{ab}	0.30 ± 0.02^b	0.38 ± 0.02^{ab}	0.622
Isoamyl alcohol [3-methylbutan-1-ol]	al3	6	1211	A, B, C	107 ± 3^a	131 ± 3^{ab}	114 ± 3^a	145 ± 10^{abc}	175 ± 22^c	160 ± 11^{bc}	113.0
1-pentanol [pentan-1-ol]	al4	9	1253	B, C	0.055 ± 0.002^{ab}	0.057 ± 0.002^{ab}	0.067 ± 0.007^a	0.046 ± 0.003^{bc}	0.035 ± 0.003^c	0.047 ± 0.002^{bc}	0.055
Prenol [3-methylbut-3-en-1-ol]	al5	10	1256	B, C	0.055 ± 0.001^a	0.054 ± 0.002^a	0.060 ± 0.008^a	0.049 ± 0.004^{ab}	0.040 ± 0.002^b	0.048 ± 0.001^{ab}	0.057
4-heptanol [heptan-4-ol]	al6	13	1283	B, C	0.081 ± 0.000^a	0.081 ± 0.001^a	0.081 ± 0.001^a	0.080 ± 00.001^a	0.080 ± 0.001^a	0.067 ± 0.002^b	0.065
4-methyl-1-pentanol [4-methylpentan-1-ol]	al7	16	1315	B, C	0.024 ± 0.001^a	0.031 ± 0.001^{abc}	0.026 ± 0.004^{ab}	0.038 ± 0.003^c	0.040 ± 0.007^c	0.036 ± 0.002^{bc}	0.021
2-heptanol [heptan-2-ol]	al8	17	1319	B, C	0.033 ± 0.001^a	0.033 ± 0.004^a	0.029 ± 0.002^a	0.035 ± 0.003^a	0.035 ± 0.002^a	0.030 ± 0.002^a	0.027
3-methylpentan-1-ol (3S)-[3-methylpentan-1-ol]	al9	18	1322	B, C	0.028 ± 0.002^a	0.025 ± 0.002^a	0.030 ± 0.006^a	0.026 ± 0.003^a	0.017 ± 0.002^a	0.027 ± 0.004^a	0.043
1-hexanol [hexan-1-oll]	al10	21	1365	A, B, C	0.070 ± 0.005^a	0.071 ± 0.009^a	0.089 ± 0.004^a	0.079 ± 0.007^a	0.079 ± 0.015^a	0.091 ± 0.006^a	0.117
cis-3-hexenol [(Z)-hex-3-en-1-ol]	al11	22	1378	B, C	0.011 ± 0.000^{ab}	0.014 ± 0.001^a	0.014 ± 0.000^b	0.014 ± 0.001^a	0.013 ± 0.002^{ab}	0.010 ± 0.000^a	0.008
3-ethoxy-1-propanol [3-ethoxypropan-1-ol]	al12	23	1379	B, C	0.103 ± 0.017^a	0.107 ± 0.021^a	0.055 ± 0.010^a	0.097 ± 0.019^a	0.078 ± 0.025^a	0.132 ± 0.042^a	0.848
trans-2-hexenol [(E)-2-hexen-1-ol]	al13	24	1394	B, C	0.075 ± 0.000^a	0.078 ± 0.001^{ab}	0.077 ± 0.001^{ab}	0.075 ± 0.001^a	0.080 ± 0.001^b	0.068 ± 0.001^c	0.064
1-heptanol [Heptan-1-ol]	al14	26	1451	B, C	0.059 ± 0.003^{ab}	0.056 ± 0.004^{ab}	0.057 ± 0.005^{ab}	0.062 ± 0.005^{ab}	0.080 ± 0.006^a	0.045 ± 0.004^b	0.217
Benzyl alcohol [Phenylmethanol]	al15	48	1872	B, C	0.67 ± 0.03^a	0.64 ± 0.04^a	1.20 ± 0.34^b	0.47 ± 0.12^a	0.29 ± 0.05^a	0.45 ± 0.03^a	0.564
2-phenethyl alcohol [2-phenylethan-1-ol]	al16	50	1912	B, C	14.9 ± 0.8^a	22.1 ± 1.5^{ab}	15.1 ± 0.9^a	27.2 ± 2.8^{ab}	33.2 ± 2.8^b	27.6 ± 4.1^{ab}	14.4
Total alcohols	Tal				139 ± 4^a	170 ± 4^{ab}	148 ± 7^a	193 ± 13^{abc}	229 ± 26^c	212 ± 16^{bc}	151
Esters											
Isoamyl acetate [3-methylbutyl acetate]	et1	2	1128	B, C	0.54 ± 0.04^a	0.44 ± 0.04^a	0.39 ± 0.09^a	0.40 ± 0.04^a	0.48 ± 0.02^a	0.47 ± 0.04^a	0.312
[Ethyl hexanoate]	et2	8	1233	B, C	0.32 ± 0.02^a	0.30 ± 0.02^a	0.30 ± 0.02^a	0.26 ± 0.02^a	0.30 ± 0.05^a	0.33 ± 0.02^a	0.264
Hexyl acetate [acetic acid hexyl ester]	et3	12	1270	B, C	0.033 ± 0.004^a	0.034 ± 0.003^a	0.040 ± 0.010^a	0.034 ± 0.008^a	0.022 ± 0.003^a	0.027 ± 0.004^a	0.021
Ethyl lactate [ethyl 2-hydroxypropanoate]	et4	20	1342	B, C	32.3 ± 1.6^{ab}	39.2 ± 1.8^{ab}	35.2 ± 2.0^{ab}	41.1 ± 2.3^{ab}	30.2 ± 6.3^a	43.4 ± 2.8^b	46.4
Ethyl caprilate [ethyl octanoate]	et5	27	1433	B, C	0.29 ± 0.01^a	0.27 ± 0.02^a	0.272 ± 0.022^a	0.26 ± 0.03^a	0.326 ± 0.03^a	0.28 ± 0.03^a	0.20
Isobutyl lactate [2-methylpropyl (2R)-2-hydroxypropanoate]	et6	29	1454	B, C	0.042 ± 0.002^a	0.059 ± 0.005^{ab}	0.054 ± 0.004^a	0.081 ± 0.012^{ab}	0.065 ± 0.008^{ab}	0.094 ± 0.010^b	0.088
[Ethyl 3-hydroxybutanoate]	et7	32	1519	B, C	1.99 ± 0.15^a	1.82 ± 0.28^a	1.55 ± 0.63^a	1.48 ± 0.09^a	1.78 ± 0.13^a	2.26 ± 00.14^a	3.52
[Ethyl 2-hydroxyhexanoate]	et8	34	1540	B, C	0.045 ± 0.004^a	0.034 ± 0.005^a	0.040 ± 0.006^a	0.035 ± 0.004^a	0.032 ± 0.006^a	0.039 ± 0.004^a	0.028
Isoamyl lactate [3-methylbutyl 2-hydroxypropanoate]	et9	36	1583	B, C	0.57 ± 0.03^a	0.76 ± 0.04^{ab}	0.80 ± 0.11^{ab}	0.69 ± 0.04^{ab}	0.76 ± 0.10^{ab}	0.94 ± 0.06^b	1.12
[Ethyl decanoate]	et10	38	1628	B, C	0.074 ± 0.008^a	0.085 ± 0.008^a	0.067 ± 0.007^a	0.095 ± 0.011^a	0.115 ± 0.013^a	0.079 ± 0.010^a	0.038
Diethyl succinate [Diethyl butanedioate]	et11	41	1674	B, C	6.73 ± 0.38^a	5.22 ± 0.53^a	4.02 ± 0.55^a	4.74 ± 0.58^a	5.86 ± 1.08^a	5.61 ± 0.80^a	3.31
Methyl salicylate [Methyl 2-hydroxybenzote]	et12	43	1763	B, C	0.083 ± 0.006^a	0.079 ± 0.012^a	0.061 ± 0.007^a	0.067 ± 0.005^a	0.083 ± 0.026^a	0.093 ± 0.014^a	0.212
Ethyl isopentyl succinate [Butanedioic acid ethyl-(3-methyl-1-butyl) ester]	et13	49	1903	B, C	0.046 ± 0.003^{ab}	0.053 ± 0.005^{ab}	0.030 ± 0.003^a	0.057 ± 0.008^{ab}	0.090 ± 0.017^c	0.066 ± 0.008^{bc}	0.037
Diethyl malate [Diethyl 2-hydroxybutanedioate]	et14	54	2045	B, C	0.33 ± 0.04^a	0.29 ± 0.02^a	0.25 ± 0.05^a	0.42 ± 0.05^a	0.41 ± 0.09^a	0.44 ± 0.06^a	0.79
Ethyl palmitate [Ethyl hexadecanoate]	et15	59	2257	B, C	0.47 ± 0.02^a	0.72 ± 0.04^{ab}	0.59 ± 0.04^{ab}	0.92 ± 0.13^b	0.80 ± 0.23^{ab}	0.79 ± 0.08^{ab}	0.73
Ethyl phenyllactate [Ethyl 2-hydroxy-3-phenylpropanoate]	et16	61	2287	B, C	0.138 ± 0.008^a	0.142 ± 0.010^a	0.124 ± 0.017^a	0.236 ± 0.029^{bc}	0.293 ± 0.034^c	0.180 ± 0.013^{ab}	0.133
Monoethyl succinate [4-ethoxy-4-oxobutanoic acid]	et17	64	2379	B, C	20.5 ± 1.1^{ab}	20.2 ± 1.9^{ab}	13.9 ± 1.6^a	18.3 ± 1.4^{ab}	26.6 ± 2.4^b	18.9 ± 1.8^{ab}	13.12
Total esters	Tet				64.5 ± 2.1^a	69.7 ± 2.5^a	57.7 ± 4.2^a	69.1 ± 3.3^a	68.2 ± 9.9^a	74.0 ± 3.9^a	70.30
Carboxylic acids											
[Acetic acid]	ac1	28	1451	B, C	3.33 ± 0.19^a	3.41 ± 0.35^a	3.54 ± 0.37^a	3.53 ± 0.45^a	3.97 ± 0.17^a	4.11 ± 0.45^a	4.93
[Propanoic acid]	ac2	33	1543	B, C	0.134 ± 0.010^a	0.160 ± 0.018^a	0.164 ± 0.035^a	0.174 ± 0.030^a	0.176 ± 0.017^a	0.161 ± 0.013^a	0.179
Isobutyric acid [2-methylpropanoic acid]	ac3	35	1562	B, C	0.227 ± 0.009^a	0.224 ± 0.018^a	0.232 ± 0.028^a	0.273 ± 0.029^a	0.259 ± 0.003^a	0.251 ± 0.022^a	0.318
Butyric acid [Butanoic acid]	ac4	37	1625	B, C	0.167 ± 0.008^a	0.151 ± 0.009^a	0.173 ± 0.030^a	0.141 ± 0.006^a	0.148 ± 0.017^a	0.176 ± 0.009^a	0.157
Isovaleric acid [3-methylbutanoic acid]	ac5	40	1663	B, C	0.39 ± 0.02^a	0.49 ± 0.03^{abc}	0.43 ± 0.04^{ab}	0.56 ± 0.05^{abc}	0.62 ± 0.07^c	0.59 ± 0.04^{bc}	0.56
Neodecanoic acid [2,2-dimethyloctanoic acid]	ac6	44	1803	B	0.92 ± 0.07^a	0.57 ± 0.05^a	0.80 ± 0.21^a	0.57 ± 0.06^a	0.68 ± 0.17^a	0.70 ± 0.07^a	0.72

Table 2 (*continued*)

Variable	Code	Peak nr	LRI$_{exp}$	ID method	UVS (24)	CVS (12)	LVS (4)	SVD (10)	GE (3)	TL (13)	TG (1)
[Hexanoic acid]	ac7	45	1838	B, C	1.18 ± 0.06^a	1.18 ± 0.08^a	1.13 ± 0.07^a	1.02 ± 0.06^a	1.12 ± 0.13^a	1.20 ± 0.08^a	1.00
[Octanoic acid]	ac8	55	2054	B, C	1.66 ± 0.07^a	1.47 ± 0.08^a	1.43 ± 0.11^a	1.49 ± 0.14^a	1.74 ± 0.14^a	1.62 ± 0.13^a	1.17
Total carboxylic acids	Tac				8.0 ± 0.2^a	7.7 ± 0.4^a	7.9 ± 0.5^a	7.7 ± 0.5^a	8.7 ± 0.2^a	8.8 ± 0.6^a	9.0
Carbonyl compounds											
Diisobutyl ketone [2,5-dimethylheptan-4-one]	cc1	5	1190	B, C	0.053 ± 0.000^a	0.053 ± 0.000^a	0.052 ± 0.001^a	0.049 ± 0.002^a	0.048 ± 0.004^a	0.036 ± 0.002^b	0.034
3-ethyl-4-heptanone [3-ethylheptan-4-one]	cc2	7	1248	B, C	0.038 ± 0.001^a	0.037 ± 0.001^a	0.038 ± 0.003^a	0.036 ± 0.001^a	0.032 ± 0.002^{ab}	0.027 ± 0.001^b	0.033
2-octanone [Octan-2-one]	cc3	14	1292	B, C	0.042 ± 0.008^a	0.062 ± 0.018^a	0.044 ± 0.012^a	0.051 ± 0.012^a	0.044 ± 0.012^a	0.093 ± 0.023^a	0.045
Amyl vinyl ketone [1-octen-3-one]	cc4	15	1297	B, C	1.99 ± 0.44^a	2.19 ± 0.40^a	2.48 ± 0.55^a	1.10 ± 0.21^a	2.62 ± 0.61^a	2.40 ± 0.80^a	4.28
[6-methylhept-5-en-2-one]	cc5	19	1336	B, C	0.117 ± 0.001^a	0.118 ± 0.001^a	0.119 ± 0.002^a	0.116 ± 0.002^a	0.101 ± 0.017^b	0.100 ± 0.003^b	0.092
Furfural [furan-2-carbaldehyde]	cc6	31	1474	B, C	0.262 ± 0.053^a	0.244 ± 0.027^a	0.257 ± 0.058^a	0.295 ± 0.103^a	0.177 ± 0.090^a	0.158 ± 0.023^a	0.182
Maltol [3-hydroxy-2-methylpyran-4-one]	cc7	51	1962	B, C	0.029 ± 0.005^a	0.034 ± 0.005^a	0.018 ± 0.006^a	0.022 ± 0.007^a	0.012 ± 0.011^a	0.020 ± 0.008^a	0.007
Glutaconic anhydride [3H-pyran-2,6-dione]	cc8	53	2024	B, C	0.085 ± 0.004^{ab}	0.094 ± 0.005^{abc}	0.064 ± 0.011^a	0.122 ± 0.010c^a	0.121 ± 0.004^c	0.114 ± 0.007^{bc}	0.101
Coumaran [2,3-dihydro-1-benzofuran]	cc9	65	2427	B, C	0.218 ± 0.021^a	0.239 ± 0.033^a	0.179 ± 0.056^a	0.263 ± 0.077^a	0.277 ± 0.025^a	0.214 ± 0.040^a	0.277
Total carbonyl compounds	Tcc				2.83 ± 0.44^a	3.07 ± 0.41^a	3.25 ± 0.47^a	2.05 ± 0.29^a	3.44 ± 0.58^a	3.17 ± 0.81^a	5.05
Phenolic compounds											
Guaiacol [2-methoxyphenol]	ph1	47	1865	B, C	0.044 ± 0.002^a	0.035 ± 0.003^{ab}	0.032 ± 0.001^{ab}	0.023 ± 0.002^b	0.022 ± 0.005^b	0.029 ± 0.003^{ab}	0.053
4-vinylguaiacol [4-ethenyl-2-methoxyphenol]	ph2	58	2194	B, C	0.128 ± 0.008^a	0.115 ± 0.013^a	0.122 ± 0.017^a	0.064 ± 0.010^a	0.061 ± 0.008^a	0.116 ± 0.030^a	0.167
Syringol [2,6-dimethoxyphenol]	ph3	60	2279	B, C	0.33 ± 0.01^a	0.29 ± 0.02^a	0.27 ± 0.03^a	0.36 ± 0.07^a	0.35 ± 0.002^a	0.29 ± 0.004^a	0.20
Isoeugenol [2-methoxy-4-(prop-1-enyl)-phenol]	ph4	63	2328	B, C	0.51 ± 0.08^a	0.66 ± 0.18^a	0.86 ± 0.32^a	0.64 ± 0.09^a	1.19 ± 0.24^a	0.85 ± 0.13^a	1.13
Vanillin [4-hydroxy-3-methoxybenzaldehyde]	ph5	66	2586	B, C	1.01 ± 0.11^a	1.20 ± 0.16^a	1.52 ± 0.34^a	1.03 ± 0.16^a	0.91 ± 0.64^a	1.09 ± 0.36^a	–
Ethyl vanillate [ethyl 4-hydroxy-3-methoxybenzoate]	ph6	69	2616	B, C	0.23 ± 0.02^{ab}	0.29 ± 0.02^a	0.30 ± 0.07^a	0.20 ± 0.03^{ab}	0.15 ± 0.03^b	0.15 ± 0.01^b	0.206
Apocynin [1-(4-hydroxy-3-methoxyphenyl)ethan-1-one]	ph7	71	2636	B, C	0.074 ± 0.002^a	0.074 ± 0.005^a	0.105 ± 0.017^b	0.057 ± 0.006^{ac}	0.046 ± 0.006^c	0.058 ± 0.002^{ac}	0.086
Total phenolic compounds	Tph				1.54 ± 0.09^a	1.70 ± 0.18^a	1.87 ± 0.47^a	1.30 ± 0.16^a	1.61 ± 0.46^a	1.38 ± 0.16^a	2.14
Lactones											
γ-Butyrolactone [dihydrofuran-2(3H)-one]	la1	39	1642	B, C	4.04 ± 0.12^a	4.29 ± 0.19^a	3.72 ± 0.20^a	4.91 ± 0.31^a	6.86 ± 2.01^{ab}	5.30 ± 0.34^b	4.644
Cis-whiskey lactone [5-butyl-4-methyldihydro-2(3H)-furanone]	la2	52	1991	B, C	0.11 ± 0.04^a	0.12 ± 0.03^a	0.11 ± 0.04^a	0.10 ± 0.02^a	0.13 ± 0.04^a	0.14 ± 0.03^a	0.06
Carboethoxy-butyrolactone [ethyl 5-oxooxolane-2-carboxylate]	la3	57	2259	B, C	0.33 ± 0.02^a	0.44 ± 0.02^a	0.35 ± 0.05^a	0.50 ± 0.06^a	0.50 ± 0.12^a	0.50 ± 0.05^a	0.51
Total lactones	Tla				4.42 ± 0.13^{ab}	4.81 ± 0.16^{ab}	4.11 ± 0.28^a	5.48 ± 0.34^{ab}	7.44 ± 1.99^{bc}	5.88 ± 0.35^c	5.213
Nitrogen compounds											
Isoamyl acetamide [N-(3-methylbutyl)acetamide]	ni1	46	1865	B, C	0.43 ± 0.06^a	1.56 ± 0.20^b	0.99 ± 0.34^{ab}	0.92 ± 0.20^{ab}	0.73 ± 0.43^a	0.72 ± 0.10^a	0.50
2-Acetamidoethyl acetate [Ethyl 2-acetamidoacetate]	ni2	56	2176	B, C	0.035 ± 0.004^a	0.035 ± 0.004^a	0.028 ± 0.003^a	0.034 ± 0.003^a	0.045 ± 0.002^a	0.034 ± 0.004^a	0.02
[N-(2-phenylethyl)acetamide]	ni3	67	2578	B, C	0.11 ± 0.02^a	0.27 ± 0.04^a	0.16 ± 0.02^a	0.20 ± 0.05^a	0.17 ± 0.06^a	0.13 ± 0.03^a	0.11
[Ethyl-5-oxopyrrolidine-2-carboxylate]	ni4	68	2632	B, C	0.44 ± 0.02^{ab}	0.44 ± 0.02^{ab}	0.58 ± 0.09^b	0.38 ± 0.06^{ab}	0.22 ± 0.06^a	0.38 ± 0.06^{ab}	0.49
Total nitrogen compounds	Tni				1.01 ± 0.08^a	2.30 ± 0.23^b	1.74 ± 0.30^{ab}	1.55 ± 0.25^{ab}	1.17 ± 0.44^a	1.27 ± 0.15^a	1.13
Sulfur compounds											
Methionol [3-(methylthio)-propan-1-ol]	su1	42	1729	B, C	0.19 ± 0.02^a	0.29 ± 0.02^{abc}	0.20 ± 0.02^{ab}	0.42 ± 0.05^{abc}	0.50 ± 0.02^c	0.44 ± 0.08^{bc}	0.18
3-methylthio-propionic acid [3-methylthio-propanoic acid]	su2	62	2316	B, C	0.186 ± 0.01^a	0.16 ± 0.02^a	0.14 ± 0.03^a	0.16 ± 0.03^a	0.17 ± 0.04^a	0.22 ± 0.09^a	0.12
Total sulfur compounds	Tsu				0.38 ± 0.02^a	0.45 ± 0.03^a	0.34 ± 0.04^a	0.59 ± 0.05^a	0.67 ± 0.06^a	0.66 ± 0.12^a	0.30
Other compounds											
Mesitylene [1,3,5-trimethylbenzene]	be1	11	1260	B, C	0.101 ± 0.001^a	0.104 ± 0.002^a	0.099 ± 0.002^a	0.097 ± 0.002^a	0.102 ± 0.003^a	0.075 ± 0.004^b	0.065
3-oxo-alpha-ionol [4-(3-hydroxybut-1-enyl)-3,5,5-trimethylcyclohex-2-en-1-one]	no1	70	2628	B, C	0.064 ± 0.004^a	0.079 ± 0.013^{ab}	0.146 ± 0.048^b	0.078 ± 0.028^{ab}	0.036 ± 0.004^a	0.056 ± 0.009^a	0.063

Notes: Peak number in GC/FID chromatogram is shown in Supplementary Material Fig. S3. Compound identification method: A: electron ionization mass spectrum (EIMS) and retention time agreed with the standard; B: EIMS agreed with those of the NIST14 mass spectral library; C: experimental retention index agreed with literature. Values are given as means ± standard errors of individual sampling sites within the same region. Means with different lowercase letters in the same row are significantly ($P < 0.05$) different based on Tukey HSD test. UVS: Upper Valais; CVS: Central Valais; LVS: Lower Valais; SVD: Southern Vaud; GE: Geneva; TL: Three Lakes; TG: Thurgau. Number of sampling sites (shown in Fig. 1) in brackets.

soil parameters—namely, fertility and rooting depth—affect the vine nitrogen status. These parameters may differ significantly among the studied wine regions.

The most important nitrogenous compounds utilized by vines are soil nitrate and ammonia, and, to a minor extent, vines use soil organic nitrogen compounds such as urea, amino acids, and peptides. Nitrogen fertilization (applied to the soils or as a foliar spray) could have been used to support the needs of the Pinot noir vines in areas where soil nitrogen content was insufficient. Other sources of differences in C/N$_{WSR}$ and δ^{15}N$_{WSR}$ can arise when making wine. To produce red wine, the grapes are crushed with their skin. This exocarp contains most of the grape nitrogen (mainly protein and breakdown products) and microorganisms, which will promote must fermentation. The indigenous microflora of grapes could differ significantly in vines grown in regions with different soils and climates. Another potential nitrogen source could be its addition (e.g., as ammonium salt) to the grape must to supplement the yeast assimilable nitrogen and prevent fermentation problems (e.g., Bell & Henschke, 2005). Consequently, the nitrogen in wines may represent a mixture of natural soil nitrogen, N-containing fertilizers, and nutrients added to the must. Since geographical information

could be obtained only from the natural soil nitrogen, the drawbacks mentioned earlier (i.e., fertilization, nutrient addition for fermentation) suggested that ^{15}N/^{14}N and C/N ratios may have poor discrimination potential. However, the δ^{15}N$_{WSR}$ and C/N values indicated three main groups of wine regions, UVS-CVS-LVS, SVD-GE, and TL (Table 2 and Fig. S1). This certain degree of arrangement of samples in groups is depicted in Fig. 2A. This grouping suggests that the eventual nitrogen fertilization or nutrient addition in the must did not mask the primary geographical ^{15}N/^{14}N and C/N signatures of grape, which appear to be preserved in the wine δ^{15}N$_{WSR}$ and C/N$_{WSR}$ values.

δ^{13}C$_{WSR}$ and δ^{15}N$_{WSR}$ were highly positively correlated ($P < 0.001$) with each other and altitude, ASMT, and HI and negatively correlated with latitude, ASTP, ASMGR, and DI (Fig. S2). C/N$_{WSR}$ was positively correlated with ASTP, ASMRH, and DI, and negatively with longitude and altitude and negatively correlated with longitude and altitude ($P < 0.001$), slope, and HI ($P < 0.01$). The correlations of δ^{13}C$_{WSR}$ and δ^{15}N$_{WSR}$ with latitude, longitude, and altitude were caused by their covariation with the climatic variables (i.e., precipitation, temperature, and relative air humidity). Altitude had the greatest influence ($r > 0.6$) on the δ^{13}C$_{WSR}$ and δ^{15}N$_{WSR}$ val-
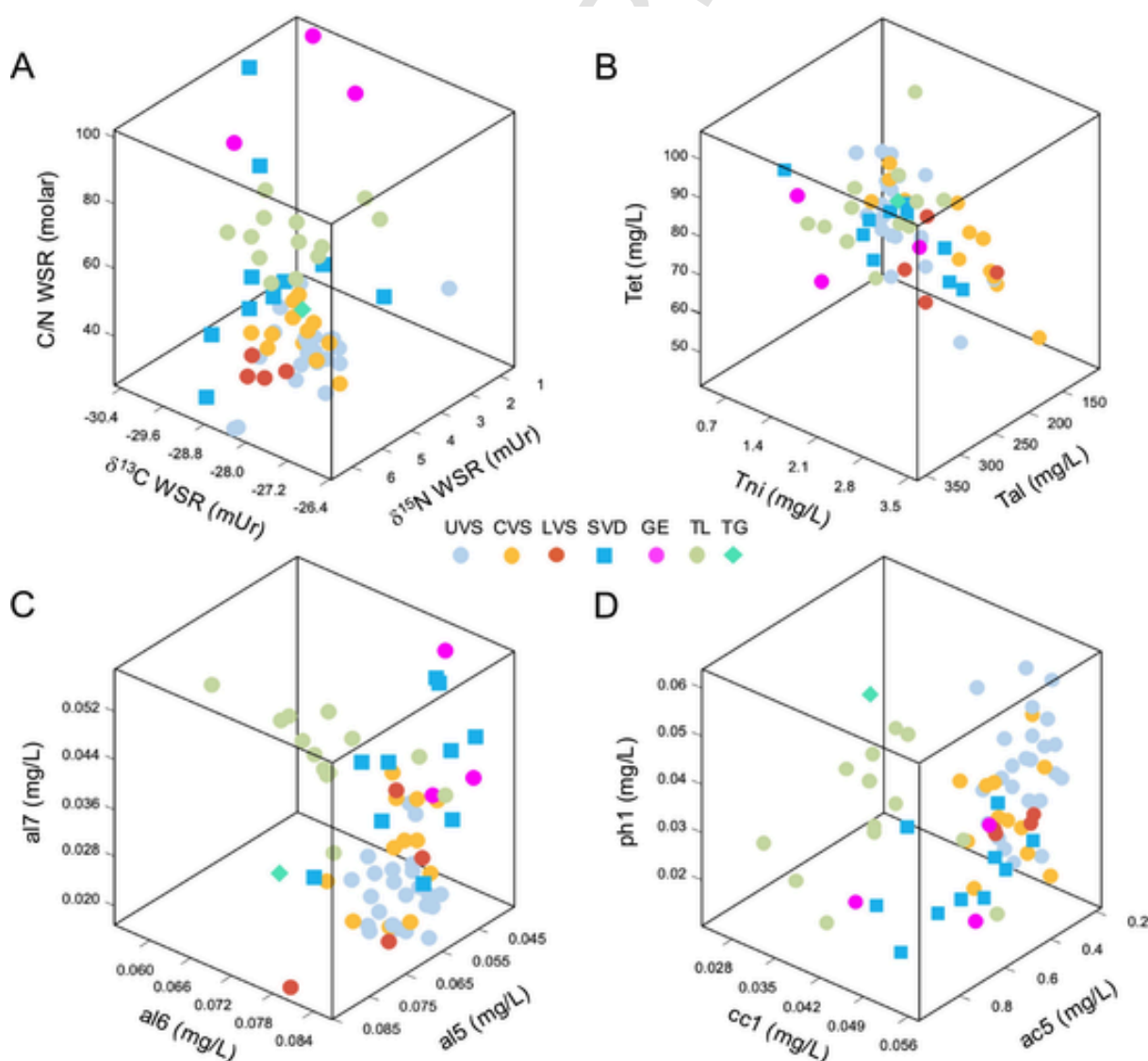

Fig. 2. Differentiation of the Pinot noir wines according to their geographical origin in three-dimensional scatter plots of δ^{13}C$_{WSR}$-δ^{15}N$_{WSR}$-C/N$_{WSR}$ (A) and concentrations of volatile organic compounds (B—D). Volatile compound code in Table 2.

ues because of its primary (vine, grape) link to vineyard soil water availability and temperature. Soil water status and temperature regulate stomatal conductance and the $^{13}C/^{12}C$ ratio of photosynthates (Flanagan & Farquhar, 2014). In water-deficient soils, soil nutrient uptake by plants is strongly reduced; soluble nitrogen (nitrate or ammonium) is less available to the vines, causing significant shifts in C/N and $\delta^{15}N$ in vine organs (Verdenal et al., 2015) and derived wine (Spangenberg & Zufferey, 2018). In summary, the $\delta^{13}C_{WSR}$, $\delta^{15}N_{WSR}$, and C/N$_{WSR}$ 3D scatterplot (Fig. 2A) and correlations with geoclimatic parameters (Fig. S2) support the hypothesis that these parameters may be used to trace Swiss Pinot noir wines.

3.3. Concentrations of volatile organic compounds

A typical gas chromatogram of the VOCs of Pinot noir wines is shown in Fig. S3. The 68 VOCs identified and semi-quantified (concentrations expressed as mg/L octan-2-ol) in all the samples included 16 alcohols, 17 esters, 8 carboxylic acids, 9 carbonyl compounds (aldehydes, ketones), 7 phenolic compounds, 3 lactones, 4 nitrogen compounds, 2 sulfur compounds, 1 benzene derivative, and 1 C$_{13}$-norisoprenoid. The IUPAC names, codes used, experimental LRI, and the mean concentrations of the VOCs expressed as the means ± standard errors of the means in the wine regions are listed in Table 2. The more abundant (> 10 mg/L) compounds were the alcohols 2-methylpropan-1-ol, 3-methylbutan-1-ol, and 2-phenylethan-1-ol, and the esters ethyl 2-hydroxypropanoate and 4-ethoxy-4-oxobutanoic acid. The next group, with concentrations between 1 and 10 mg/L, included ethyl 3-hydroxybutanoate, diethyl butanedioate, acetic acid, hexanoic acid, octanoic acid, 1-octen-3-one, 4-hydroxy-3-methoxybenzaldehyde, and dihydrofuran-2(3H)-one. The individual VOC concentrations and the total contents of the VOC classes (i.e., Tal, Tet, Tac, Tcc, Tph, Tla, Tni, and Tsu) were consistent with previously reported values for Pinot noir wines (Longo et al., 2021 and references therein). These VOCs were derived from the grape berry exocarp and mesocarp during yeast- and bacteria-mediated fermentation and aging in oak barrels, stainless steel containers, and glass bottles. The C$_6$-alcohols, esters, and carbonyl compounds were the dominant aroma compounds in Pinot noir berries and affected mainly the green/fresh, fruity flavor of the derived wine; the C$_{13}$-norisoprenoids contributed to the fruity aroma of the wine (Fang & Qian, 2006; Herrero et al., 2016). A compound-specific $\delta^{13}C$ study of the 18 most abundant VOCs in Pinot noir wines specified or confirmed their biosynthetic origin and pathways during winemaking and aging (Spangenberg et al., 2017). Interestingly, the acetic acid concentrations were similarly low in all the wines from the different regions, except two outliers with 7.0 and 8.2 mg/L. These results indicated that limited oxidation and no microbial spoilage occurred during winemaking or the two years (2013–2015) of storage in bottles.

The one-way ANOVA results (Table 2) and boxplots (data not shown for brevity) revealed that the total concentrations of alcohols, lactones, and nitrogen compounds and 36 individual VOCs were significantly different ($F > 0.1$, $P < 0.05$) among at least one of the wine-growing areas. The total alcohol and lactone contents were higher in SVD, GE, and TL than in the Valais regions. A minimal separation of the wine regions is shown in the three-dimensional scatterplot based on total alcohols, esters, and carboxylic acids (Fig. 2B). However, the 3D scatterplots based on the concentrations of individual VOC compounds reveal a better separation of regions, as shown in for heptan-4-ol-3, methylbut-3-en-1-ol, and 4-methylpentan-1-ol (Fig. 2C) and for 2,6-dimethylheptan-4-one, 3-methylbutanoic acid, and 2-methoxyphenol (Fig. 2D). The Valais wines had higher concentrations in 2-methoxyphenol, ethyl 4-hydroxy-3-methoxybenzoate, 1-(4-hydroxy-3-methoxyphenyl)ethan-1-one, 3-ethylheptan-4-on3, 6-methylhept-5-en-2-one, ethyl-5-oxopyrrolidine-2-carboxylate, 1,3,5-trimethylbenzene, and 4-[(E)-3-hydroxybut-1-enyl]-3,5,5-trimethylcyclohex-2-en-1-one, and lower concentrations of 2-methylpropyl (2R)-2-hydroxy propanoate, ethyl 2-

hydroxy-3-phenylpropanoate, dihydrofuran-2(3H)-one, ethyl 5-oxooxolane-2-carboxylate, 3-methylthio-propan-1-ol, and 3H-pyran-2,6-dione than the wines from other regions (Table 2). The LVS wines had VOC profiles similar to those of SVD and GE. The SVD wines had lower 1-octen-3-one and 2-methoxy-4-(prop-1-enyl)-phenol contents than those from GE (Table 2). The samples from the TL region had high 2-methylpropan-1-ol and 3-methylbutyl 2-hydroxypropanoate contents and low heptan-4-ol, (Z)-hex-3-en-1-ol, (E)-2-hexen-1-ol, heptan-1-ol, and 3-ethylheptan-4-one contents. Notably, the TL samples PN54 and PN55, which were from site 22 on the southern shore of Lake Neuchâtel in the Canton of Vaud (Fig. 1), plot near the SVD wines in the scatterplots of Fig. 2. Finally, it is not surprising that there were relatively small differences in the semi-quantitative concentrations of VOCs between the regions. The VOCs in grape and wine are qualitatively and quantitatively dependent on environmental conditions and viticultural and oenological factors, whose combined action is poorly understood (e.g., Tassoni, Tango, & Ferri, 2013). Nevertheless, despite the variations in environment and practices, general trends were observed from the ANOVA results, which were confirmed by PCA and LDA models (see Section 3.4).

Several VOCs were significantly correlated ($P < 0.01$) with each other and with geographical coordinates, climatic parameters, bioclimatic indices, $\delta^{13}C_{WSR}$, $\delta^{15}N_{WSR}$, and C/N$_{WSR}$ (Fig. S2). Particularly, two alcohols and three esters (a1, a12, et4, et6, and et9, compound codes in Table 2) were highly positively correlated ($P < 0.001$) with latitude, ASTP, ASMRH, and DI and negatively correlated with longitude, altitude, and HI. Three alcohols, three carbonyl compounds, and 1,3,5-trimethylbenzene (al6, al11, al13, cc1, cc2, cc5, and be1) were highly negatively correlated ($P < 0.001$) with latitude, ASTP, ASMRH, and DI and positively correlated with altitude, ASMT, and HI (Fig. S2). The covariation between the VOCs and the geographical coordinates and altitude (i.e., site elevation), like those of $\delta^{13}C_{WSR}$, $\delta^{15}N_{WSR}$, and C/N$_{WSR}$, was most likely due to their close link with precipitation (i.e., soil water availability) and temperature. These findings aligned with the recently reported correlations of the sensorial qualifiers (aroma, taste, and mouthfeel) of Pinot vines from the US west coast with latitude and longitude (Cantu et al., 2021).

3.4. Multivariate analyses for the geographical characterization of Swiss Pinot noir wines

3.4.1. Exploratory analysis with PCA

The pattern of covariation between volatiles and isotopic variables and their link to the geographical origin of the wines was further evaluated with principal component analysis. The variables that best differentiate the wines from different regions were selected based on the one-way ANOVA results (Table 2), Pearson's correlation coefficients (Fig. S2), and patterns in scatterplots (Fig. 2) and boxplots (Fig. S1) for PCA. Several PCA tests were performed with a combination of subsets of variables. Their quality was assessed by studying the clustering of sample scores in 3D scatter plots and the reduction of dimensionality and explained variance in scree plots. The selected variable included $\delta^{13}C_{WSR}$, $\delta^{15}N_{WSR}$, C/N$_{WSR}$, and 20 VOCs (al1, al3, al5, al6, al7, al13, al16, et6, et9, et15, et16, cc1, cc2, cc5, cc8, ph1, ph7, ni4, su1, and be1, compound codes in Table 2). The first three principal components (PC1–3) explained 64.8 % of the cumulative variance. The clustering of the variables and their relative influence on the components is presented in a scatterplot of the ladings (Fig. 3A). The variables highly correlated to the components were ordered in decreasing absolute loading values (> 0.4) for components PC1 (negatively with cc1, $\delta^{15}N_{WSR}$, al6, cc2, be1, cc5, $\delta^{13}C_{WSR}$, ph1, ph7, al13, al15 and positively with al3, su1, et6, al7, al16, C/N$_{WSR}$, al1, cc8, et15, et9, et16), PC2 (positively with cc1, al6, al7, be1, C/N$_{WSR}$, cc5, et16, al13), and PC3 (positively with ph7, ni4, al5). Positive loading indicates that the variable contributed to the principal component, and negative loading reflects that the variable con-
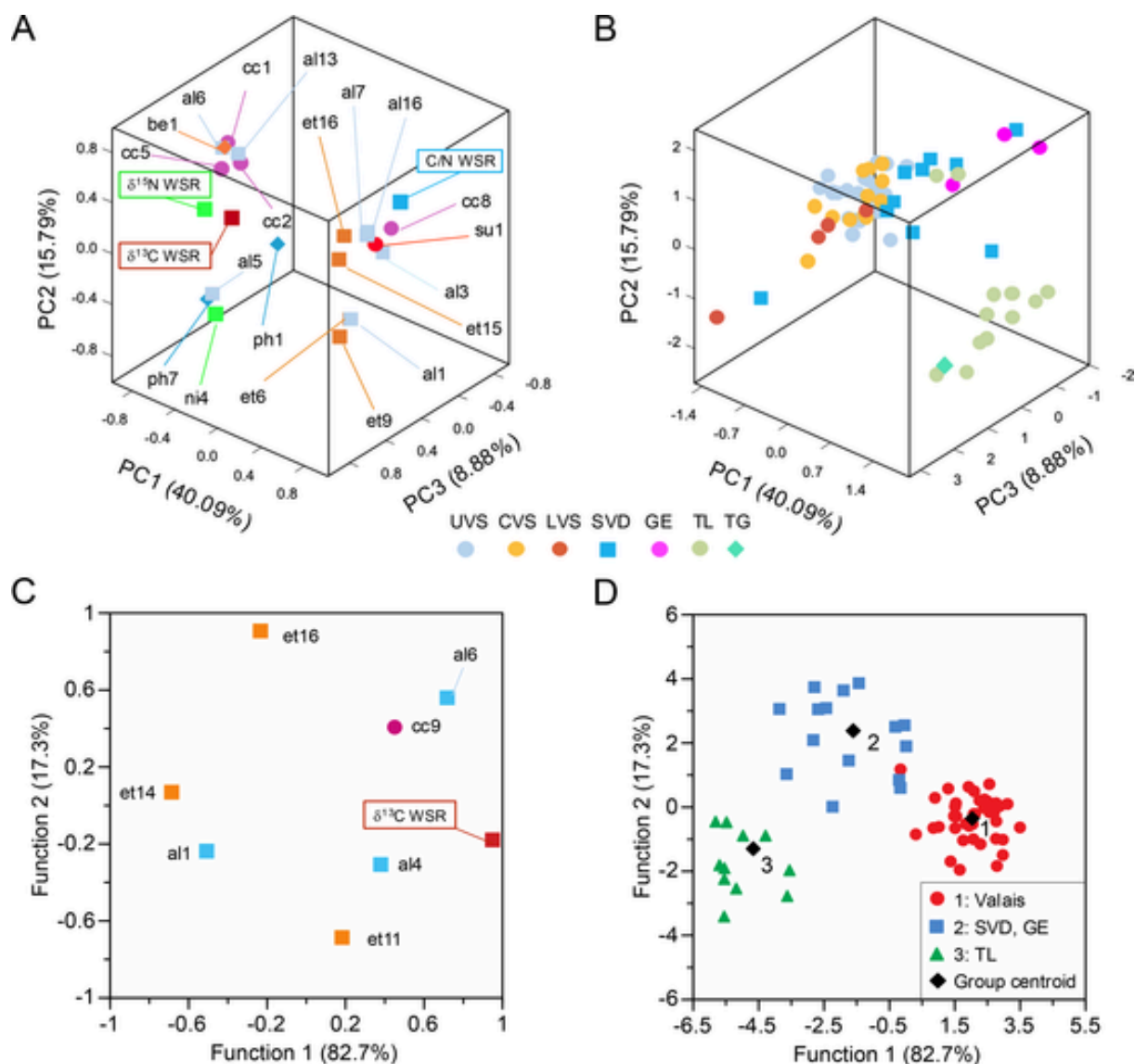
Fig. 3. Scatter plots of loadings and scores of principal component analysis (A, B) and classification function coefficients and scores of linear discriminant analysis model (C, D) performed on Pinot noir wines from different regions in Switzerland (Fig. 1). The variables include carbon and nitrogen isotope and molar ratios of wine solid residues and volatile organic compound concentrations. Volatile compound code in Table 2.

tributed by its absence. In particular, $\delta^{15}N_{WSR}$ and $\delta^{13}C_{WSR}$ were highly negatively correlated with PC1 (−0.71 and − 0.59), and C/N_{WSR} was highly positively correlated with PC1 and PC2 (0.63 and 0.47). The arrangement of wine samples in the scatterplot of the PC scores shows that PC1 and PC2 seem to separate the wines samples from Valais and SVD from those in TL and TG; PC2 and PC3 separated the LVS and SVD wines from those in GE (Fig. 3B). Samples PN54 and PN55 from the northern Vaud appear within the cluster of TL samples, which is correct in the classification of Swiss wine-growing regions.

3.4.2. Classification analysis with LDA

The PCA scores suggested that the wine samples can be classified into three groups, corresponding to the suggested zones based on geoclimatic and bioclimatic differences: Valais, southern Vaud-Geneva, and Three Lakes-Thurgau. The wines from these regions were classified via linear discriminant models using as independent variables the isotopic and molar ratios ($\delta^{13}C_{WSR}$, $\delta^{15}N_{WSR}$, and C/N_{WSR}) and the volatile data (concentrations of 68 individual VOCs and eight total concentrations of VOC classes). A stepwise procedure was used to select variables

that effectively discriminate between the wines while excluding redundant information to minimize the model dimension. The selection criterion used Wilk's lambda (λ_w) test statistics, with λ_w values in the 0–1 range, where $\lambda_w = 0$ for perfect separation of the groups and $\lambda_w = 1$ for no discrimination. Stepwise, a variable was added or removed; the variable that minimizes the overall λ_w was retained at each step, otherwise excluded. The significance of the change in λ_w when a variable was added or removed was measured with an F test ($F > 3.84$ to enter and $F < 2.71$ to be removed). The maximum number of functions was the number of groups minus one. The canonical discriminant functions were determined by maximizing the variances of the variables between groups and minimizing them within each group. The standardized canonical coefficient gives the importance of each variable in the discriminant function; the higher the absolute value, the greater the relative contribution to the overall discrimination. The first stepwise LDA examined the classification of the wines into the three groups suggested by PCA (the sample from Thurgau was excluded). A subset of eight variables was selected, including heptan-4-ol, ethyl 2-hydroxy-3-phenylpropanoate, $\delta^{13}C_{WSR}$, diethyl 2-hydroxybutanedioate, 2-

methylpropan-1-ol, 2,3-dihydro-1-benzofuran, diethyl butanedioate, and pentan-1-ol in order of decreasing discrimination power (overall $\lambda_w = 0.044$, Fig. 3C). Functions 1 and 2 explained 82.7 % and 17.3 % of the variance, respectively. The recognition ability (correct classification of the samples to the group) and prediction ability (cross-validation of the samples to the group) were 92.4 % and 89.4 %, respectively. Among the seven misclassified samples were PN54 and PN55, which were predicted to belong to the southern Vaud-Geneva group instead of the Three Lakes group. Considering the actual geographical origin of these samples in the canton of Vaud, the other samples from Three Lakes formed a group labeled Fribourg-Neuchâtel-Bern (see Fig. 1 for location). Consequently, the three wine sample groups finally retained were Valais, Vaud-Geneva, and Fribourg-Neuchâtel-Bern. A stepwise LDA performed on this samples grouping selected nine variables, including heptan-4-ol, 2,6-dimethylheptan-4-one, ethyl 2-hydroxy-3-phenylpropanoate, $\delta^{13}C_{WSR}$, 2,3-dihydro-1-benzofuran, $\delta^{15}N_{WSR}$, diethyl butanediote, pentan-1-ol, and 2-methoxyphenol ($\lambda_w = 0.012$, Fig. 4A). Functions 1 and 2 explained 82.6 % and 17.4 % of the variance, respectively. The classification performance was improved to 97.0 % recognition accuracy and 95.5 % prediction accuracy. The wines from Fribourg-Neuchâtel-Bern were effectively separated from those from Valais and Vaud-Geneva (Fig. 4B). The last two groups contained three misclassified wines, which were from sites near the boundary between the lower Valais-Vaud and Vaud-Fribourg regions.

To evaluate the separate contributions of isotopes and volatiles on the discrimination potential, LDAs were performed using as variables the carbon and nitrogen isotopic and molar ratios and another with concentrations of the volatile compounds. The sample groups were Valais, Vaud-Geneva, and Fribourg-Neuchâtel-Bern. The LDA using $\delta^{13}C_{WSR}$, $\delta^{15}N_{WSR}$, and C/N$_{WSR}$ resulted in poor discrimination ($\lambda_w = 0.638$), decreasing per variable in the order $\delta^{13}C_{WSR} \approx \delta^{15}N_{WSR} >$ C/N$_{WSR}$ and low recognition and prediction abilities (89.4 % and 84.8 %). In the stepwise LDA model using only VOCs, nine of them were selected. They had a discrimination ability decreasing in the order pentan-1-ol, heptan-4-ol, ethyl 2-hydroxy-3-phenylpropanoate, total esters, 2,5-dimethylheptan-4-one, 2,3-dihydro-1-benzofuran, 2-methoxyphenol, 4-ethenyl-2-methoxyphenol, and 1,3,5-trimethylbenzene ($\lambda_w = 0.017$). Functions 1 and 2 explained 86.0 % and 14.0 % of the variance, respectively. The recognition and prediction accuracies increased to 95.5 % and 90.9 %, respectively, but were lower than those obtained when combining VOCs with isotopes (i.e., 97.7 % and 95.5 %).

Finally, we investigated whether focusing on smaller regions would enhance the prediction accuracy of the discriminant model. We first tested if a stepwise LDA model could effectively differentiate among the Valais subregions (UVS, CVS, and LVS, $n = 40$ samples). Eight variables were selected based on their discriminating capacity, listed in order of importance: total nitrogen compounds, 4-methylpentan-1-ol, phenylmethanol, ethyl 2-hydroxy-3-phenylpropanoate, $\delta^{13}C_{WSR}$, 3-methylbutyl 2-hydroxypropanoate, total esters, and ethyl 4-hydroxy-3-methoxybenzoate ($\lambda_w = 0.041$, Fig. 4C). The recognition and prediction abilities were 97.5 % and 92.5 %, respectively (Fig. 4D). We then tested the possible separation of lower Valais, southern Vaud, and Geneva regions. The stepwise LDA selected three variables, C/N$_{WSR}$, 1-octen-3-one, and (E)-2-hexen-1-ol, none of them were retained in the previous LDAs ($\lambda_w = 0.086$, Fig. 4E–F). The model showed a recognition capability of 100 % and a prediction ability of 94.1 %. The high discrimination powers of the last two models (Fig. 4C–F) showed that LDA performed better when the model is of small size and a low complexity. These models identified unique markers for the geographical
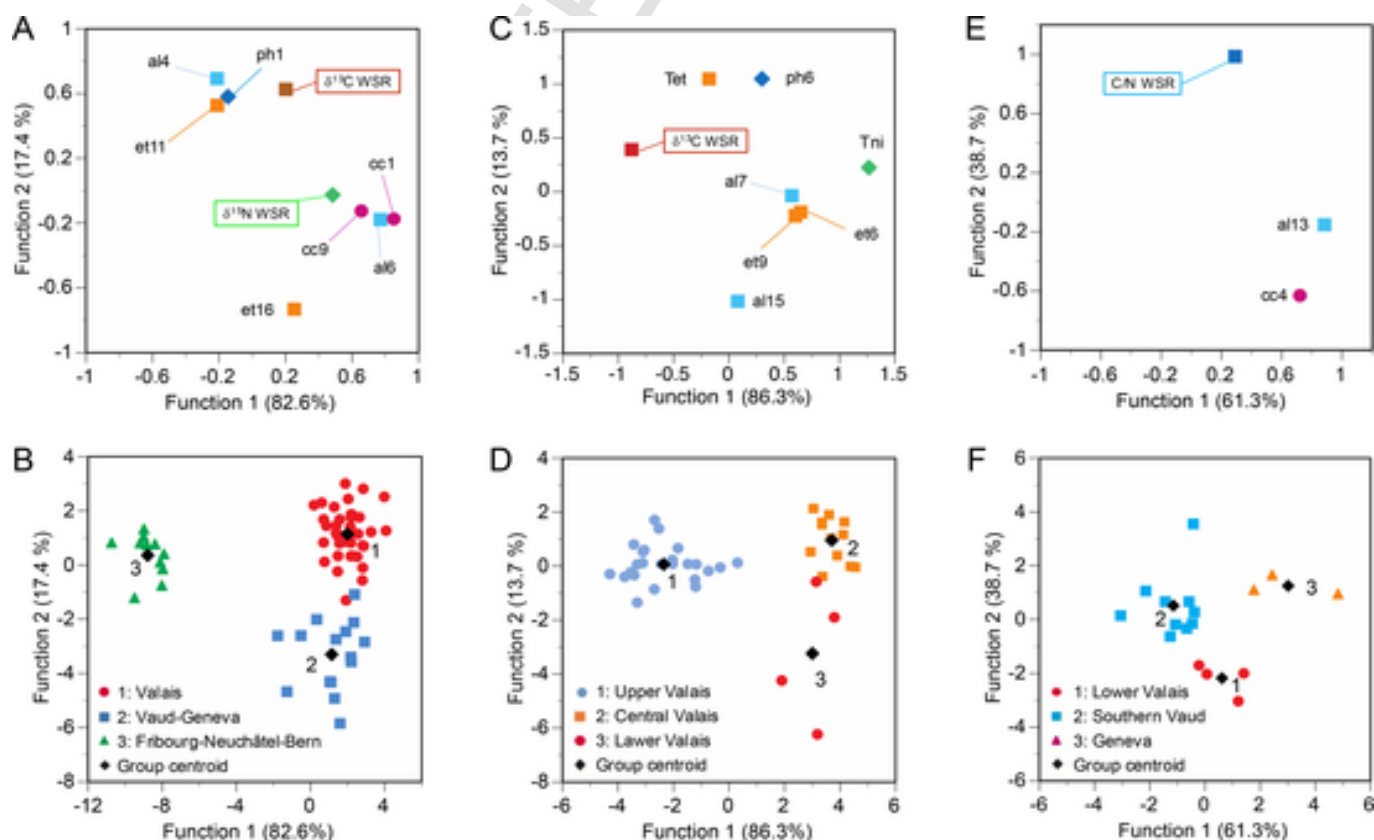

Fig. 4. Classification function coefficients and scores of linear discrimination analysis models for Pinot noir wines grouped according to the canton of origin (A, B), differentiating between subregions in the canton of Valais (C, D), and lower Valais-southern Vaud-Geneva (E, F); see site location in Fig. 1. The variables include carbon and nitrogen isotope and molar ratios of wine solid residues and volatile organic compound concentrations. Volatile compound code in Table 2.

discrimination of Pinot noir wines in subregions of southwestern Switzerland.

3.4.3. Link between geographical origin with soil parameters

We examined the potential connection between the geographical classification of wines based on $\delta^{13}C_{WSR}$, $\delta^{15}N_{WSR}$, C/N_{WSR}, and VOCs and factors thought to influence their geographical fingerprinting ability. We considered the effects of vineyard soil characteristics, particularly carbonate content and stoniness, and the aging of wines in oak barrels or stainless steel containers. Calcareous soils are alkaline and are frequently characterized by low availability of plant nutrients, such as P, N, K, Fe, Zn, and Cu, due to their low solubility at high pH and formation of precipitates or insoluble complexes (Bolan et al., 2023). These soil nutrient deficiencies can affect vine growth and yield and the quantity and quality of the grape and derived wines (e.g., Amorós et al., 2018; Blotevogel et al., 2019; Grainger et al., 2021; Palma-López, Sánchez-Rodríguez, del Campillo, León-Gutiérrez, & Ramírez-Pérez, 2024). A stepwise LDA was performed on the wines grouped according to the carbonate content of the vineyard soil (highly calcareous, moderately calcareous, and noncalcareous). Only two variables were retained: 2-methoxyphenol (guaiacol) and N-(3-methylbutyl)acetamide

(λ_w = 0.450). Functions 1 and 2 explained 71.2 % and 28.8 % of the variance, respectively (Fig. 5A). The recognition and prediction abilities were low (72.7 % and 71.2 % respectively). Function 1 separated the wines from highly calcareous soils from those of noncalcareous and moderately calcareous soils (Fig. 5B). Wines from moderately calcareous and noncalcareous soils are poorly separated by function 2. Stepwise LDA was then used to build classifiers for wines according to vineyard soil stoniness (not stony, stony, very stony, or extremely stony). The variables selected were $\delta^{13}C_{WSR}$ and eight VOC concentrations, including guaiacol and N-(3-methylbutyl)acetamide (λ_w < 0.05; Fig. 5C). Three functions explained 80.6 %, 14.2 %, and 5.2 % of the total variance, respectively. Functions 1 and 2 separated the not stony from the extremely stony samples but could not distinguish the stony from very stony samples (Fig. 5D). The recognition and prediction abilities were 86.4 % and 71.2 %, respectively. These low abilities are consistent with the results of studies by van Leeuwen, Roby, and de Rességuier (2018), suggesting that climate had a stronger influence on grape composition than soil type, regardless of whether it is gravelly, clayey, or sandy.

It is worth noting that N-(3-methylbutyl)acetamide and guaiacol were discriminating variables in the LDA models on soil parameters. The relationships between N-(3-methylbutyl)acetamide with the soil
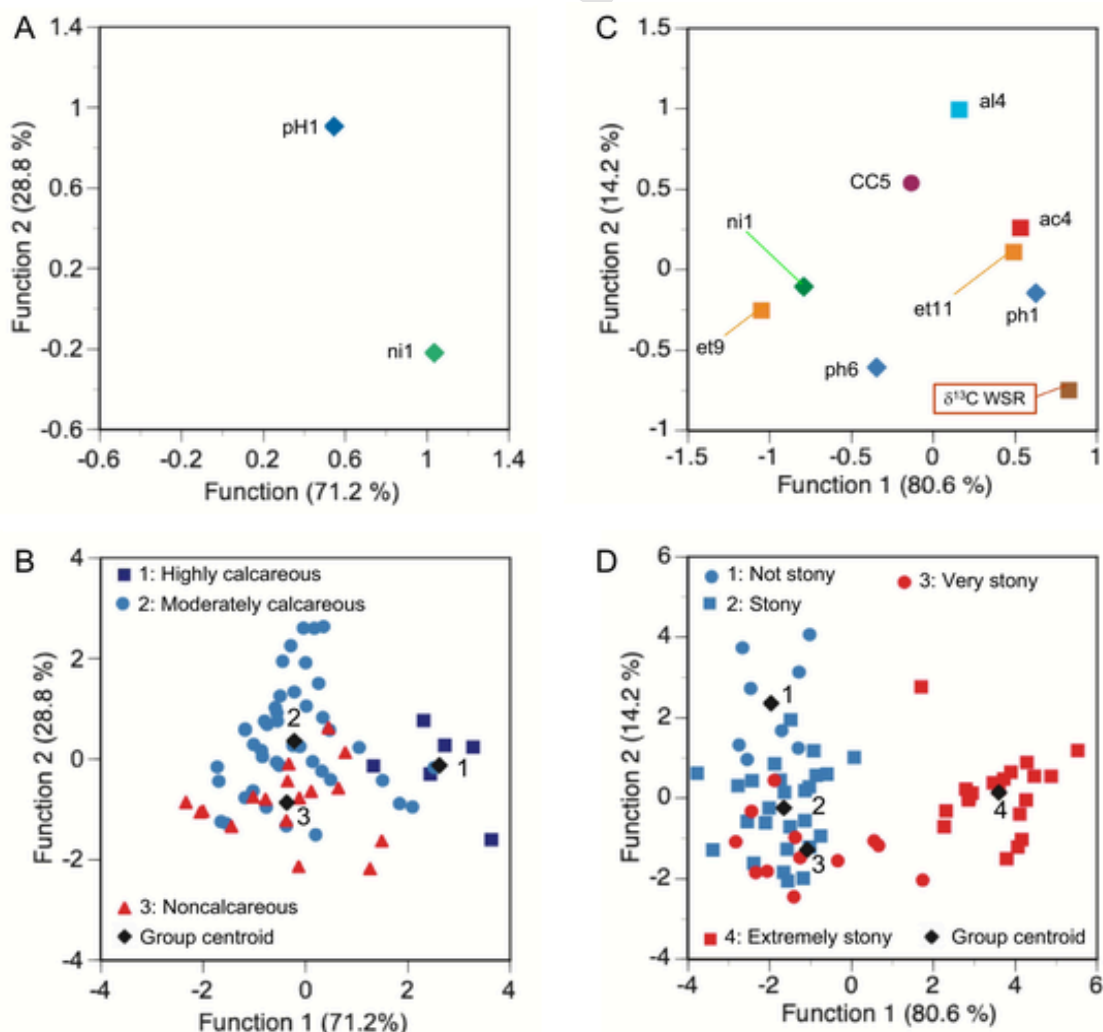

Fig. 5. Classification function coefficients and scores of linear discrimination analysis models for Pinot noir wines grouped according to the soil carbonate content (A, B) and soil stoniness (C, D) in sites from southwestern Switzerland (Fig. 1). The variables include carbon and nitrogen isotope and molar ratios of wine solid residues and volatile organic compound concentrations. Volatile compound code in Table 2.

calcareous content (i.e., soil pH) and stoniness (i.e., soil water drainage) were most likely because these soil factors determine the microorganisms present in the grapes. Recently, it was shown that the microbial community structure in the soil and rhizosphere of Pinot noir vineyards differ between regions and that these differences are preserved in the wines (Gamalero et al., 2020). A high level of N-(3-methylbutyl)acetamide indicates the presence of wild yeast in botrytized grapes; therefore, this compound was classified as a low-typicity marker negatively correlated with wine quality (Sherman, Coe, Grose, Martin, & Greenwood, 2020). This acetamide, together with guaiacol, gives a smoky note, and their concentrations were found to increase with increased maceration/fermentation grape-skin contact time (Wang, Gambetta, & Jeffery, 2016). Guaiacol and other organoleptic volatile phenols in wines may originate from various origins, including grapes exposed to smoke, heat-treated oak barrels, spoilage yeast *Brettanomyces bruxellensis*, and endogenous metabolic pathways (Noestheden, Noyovitz, Riordan-Short, Dennis, & Zandberg, 2018). The possibility of exogenous guaiacol sources, such as smoke or oak barrels, in the studied Pinot noir wines should not be overlooked. Additionally, in medium-calcareous environments, mild to moderate iron deficiency (iron chlorosis) can increase concentrations of some volatile compounds, including guaiacol (Sánchez et al., 2022).

The functions of the LDA model for the wines grouped according to the abundance of carbonate minerals and stones in the vineyard soils showed correlations ranging from marginally ($r < 0.40$) to significantly ($r < 0.50$, $P < 0.001$) with those of the geographical origin models (Fig. S4). These correlations and the principal and discriminant analyses suggest that geographical location and environmental factors—such as geoclimatic and bioclimatic parameters, and soil water availability, and to a much lesser extent soil stoniness and carbonate content—impact wine volatile profiles and isotopic ratios of solid residues. These findings validate the effectiveness of the proposed approach for traceability of wines and confirm the hypotheses of this study. However, there were some limitations to this study. First, although the semi-quantitative volatile compounds show clear relationships with the wine origin, the quantitative data could provide further insights. Secondly, this study focused on regions in southwestern Switzerland; therefore, future research should include Pinot noir wines from northwestern and central Switzerland and test the applicability of the proposed approach to wine regions worldwide.

3.4.4. Link between geographical origin with oak aging

Finally, the effect of aging in oak barrels or stainless-steel tanks on the geographical classification based on isotopes and volatiles was evaluated using ANOVA and GLM. The effects of the factors (geographical origin and aging container type) and their interactions on all the variables are shown in Table S4. The type of container marginally affected ($P = 0.051$) the $\delta^{15}N_{WSR}$ and significantly affected ($P < 0.05$) the concentrations of nine VOCs, including total lactones ($P = 0.004$), dihydrofuran-2(3H)-one ($P = 0.009$), furan-2-carbaldehyde ($P = 0.019$), total esters ($P = 0.009$), acetic acid ($P = 0.023$), total carbonyl compounds (0.023), ethyl lactate ($P = 0.027$), (E)-2-hexen-1-ol ($P = 0.032$), and 4-ethenyl-2-methoxyphenol ($P = 0.040$). The interactions between the factors did not affect the isotopic ratios in solid residues nor the concentrations of most volatile compounds at the 95 % confidence level. The exceptions were ethyl decanoate, methyl salicylate, and octanoic acid ($P < 0.05$).

4. Conclusions

Here, for the first time, the isotopic and molar ratios of carbon and nitrogen in solid residues, alone or combined with VOC abundances, demonstrated the ability to discriminate the geographical origin of wines. The 67 Pinot noir wines from 30 different areas in southwestern Switzerland showed an extensive range of variations in $\delta^{12}C_{WSR}$ (4.3

mUr), $\delta^{15}N_{WSR}$ (6.1 mUr), and C/N$_{WSR}$ (77). These parameters and 38 out of 68 VOC concentrations revealed significant differences between wines when grouped in six regions. These differences were related to altitude, precipitation, temperature, and air humidity. PCA clustered the wines from the six regions into three main groups. The validity of this classification was confimed through a stepwise LDA model built on $\delta^{13}C_{WSR}$, $\delta^{15}N_{WSR}$, and seven VOCs (prediction ability of 95.5 %). Further group-specific stepwise LDAs performed on a smaller set of samples from subregions and other selected variables achieved prediction performances > 90 %. These models included at least one of the molecular and isotopic ratios. Hence, the first hypothesis that $\delta^{12}C_{WSR}$, $\delta^{15}N_{WSR}$, and C/N$_{WSR}$ are discriminating variables for the geographical traceability of wines is proven. Finally, two-way analyses of variance provide insights into the other hypotheses, revealing that soil factors (stoniness, carbonate content) and 3–6 months of aging in oak barrels do not interact with the classification of the geographical origin of wines in this study. Further studies should focus on various wine varieties, geographical regions, vintage years, and also long-term aging in oak barrels to validate the efficacy of the proposed approach for wine traceability.

CRediT authorship contribution statement

Jorge Enrique Spangenberg: Writing – review & editing, Writing – original draft, Visualization, Methodology, Investigation, Formal analysis, Data curation, Conceptualization. **Julien Baumann:** Writing – review & editing, Methodology, Investigation. **Vivian Zufferey:** Writing – review & editing, Methodology, Investigation, Conceptualization.

Uncited reference

Declaration of competing interest

The authors declare that they have no known competing financial interests or personal relationships that could have appeared to influence the work reported in this paper.

Data availability

All data for this paper are within the manuscript and its Supplementary Information.

Appendix A. Supplementary data

Supplementary data to this article can be found online at https://doi.org/10.1016/j.foodchem.2025.145147.

References

Amorós, J.A., Bravo, S., Pérez-De-Los-Reyes, C., García-Navarro, F.J., Campos, J.A., Sánchez-Ormeno, M., … Hugueras (2018). Iron uptake in vineyard soils and relationships with other elements (Zn, Mn and ca). The case of Castilla-La Mancha, Central Spain. *Applied Geochemistry*, *88*, 17–22. https://doi.org/10.1016/j.apgeochem.2017.02.009.

Ayestarán, B., Martínez-Lapuente, L., Guadalupe, Z., Canals, C., Adell, E., & Vilanova,

M. (2019). Effect of the winemaking process on the volatile composition and aromatic profile of Tempranillo Blanco wines. *Food Chemistry*, *276*, 187–194. https://doi.org/10.1016/j.foodchem.2018.10.013.

Beck, H.E., McVicar, T.R., Vergopolan, N., Berg, A., Lutsko, N.J., Dufour, A., et al. (2023). High-resolution (1 km) Köppen-Geiger maps for 1901-2099 based on constrained CMIP6 projections. *Scientific Data*, *10*, 724. https://doi.org/10.1038/s41597-023-02549-6.

Bell, S.J., & Henschke, P.A. (2005). Implications of nitrogen nutrition for grapes, fermentation and wine. *Australian Journal of Grape and Wine Research*, *11*, 242–295. https://doi.org/10.1111/j.1755-0238.2005.tb00028.x.

Blotevogel, S., Schreck, E., Laplanche, C., Besson, P., Saurin, N., Audry, S., et al. (2019). Soil chemistry and meteorological conditions influence the elemental profiles of west European wines. *Food Chemistry*, *298*, 125033. https://doi.org/10.1016/j.foodchem.2019.125033.

Bolan, N., Srivastava, P., Rao, C.S., Satyanaraya, P.V., Anderson, G.C., Bolan, S., et al. (2023). Distribution, characteristics and management of calcareous soils. In D. L. Sparks (Ed.). *Advances in Agronomy*, *182*, 80–129. https://doi.org/10.1016/bs.agron.2023.06.002.

Calderone, G., & Guillou, C. (2008). Analysis of isotopic ratios for the detection of illegal watering of beverages. *Food Chemistry*, *106*(4), 1399–1405. https://doi.org/10.1016/j.foodchem.2007.01.080.

Camin, F., Dordevic, N., Wehrens, R., Neteler, M., Delucchi, L., Postma, G., & Buydens, L. (2015). Climatic and geographical dependence of the H, C and O stable isotope ratios of Italian wine. *Analytica Chimica Acta*, *853*, 384–390. https://doi.org/10.1016/j.aca.2014.09.049.

Cantu, A., Lafontaine, S., Frias, I., Sokolowsky, M., Yeh, A., Lestringant, P., et al. (2021). Investigating the impact of regionality on the sensorial and chemical aging characteristics of pinot noir grown throughout the US west coast. *Food Chemistry*, *337*, 127720. https://doi.org/10.1016/j.foodchem.2020.127720.

Casassa, L.F., Huff, R., & Steele, N.B. (2019). Chemical consequences of extended maceration and post-fermentation additions of grape pomace in pinot noir and zinfandel wines from the central coast of California (USA). *Food Chemistry*, *300*, 125147. https://doi.org/10.1016/j.foodchem.2019.125147.

Evans, J.R., & von Caemmerer, S. (2013). Temperature response of carbon isotope discrimination and mesophyll conductance in tobacco. *Plant, Cell & Environment*, *36*, 745–756. https://doi.org/10.1111/j.1365-3040.2012.02591.x.

Fang, Y., & Qian, M.C. (2006). Quantification of selected aroma-active compounds in pinot noir wines from different grape maturities. *Journal of Agricultural and Food Chemistry*, *54*(22), 8567–8573. https://doi.org/10.1021/jf061396m.

Ferreira, V., López, R., Escudero, A., & Cacho, J.F. (1998). Quantitative determination of trace and ultratrace flavour volatile compounds in red wines through gas chromatographic-ion trap mass spectrometric analysis of microextracts. *Journal of Chromatography A*, *806*, 349–354. https://doi.org/10.1016/S0021-9673(98)00070-3.

Flanagan, L.B., & Farquhar, G.H. (2014). Variation in the carbon and oxygen isotope composition of plant biomass and its relationship to water-use efficiency at the leaf- and ecosystem-scales in a northern Great Plains grassland. *Plant, Cell & Environment*, *37*, 425–438. https://doi.org/10.1111/pce.12165.

Gamalero, E., Bona, E., Novello, G., Boatti, L., Mignone, F., Massa, N., et al. (2020). Discovering the bacteriome of *Vitis vinifera* cv. Pinot noir in a conventionally managed vineyard. *Scientific Reports*, *10*, 6453. https://www.nature.com/articles/s41598-020-63154-w.

Grainger, C., Yeh, A., Byer, S., Hjelmeland, A., Lima, M.M.M., & Runnebaum, R.C. (2021). Vineyard site impact on the elemental composition of pinot noir wines. *Food Chemistry*, *334*, 127386. https://doi.org/10.1016/j.foodchem.2020.127386.

Herrero, P., Sáenz-Navajas, P., Culleré, L., Ferreira, V., Chatin, A., Chaperon, V., et al. (2016). Chemosensory characterization of chardonnay and pinot noir base wines of champagne. Two very different varieties for a common product. *Food Chemistry*, *207*, 239–250. https://doi.org/10.1016/j.foodchem.2016.03.

van Leeuwen, C., Roby, J.-P., & de Rességuier, L. (2018). Soil-related terroir factors: A review. *OENO one*, *53*(2), 173–188. https://doi.org/10.20870/oeno-one.2018.52.2.2208.

van Leeuwen, C., Sguibn, G., Bois, B., Ollat, N., Swingedouw, D., Zito, S., & Gambetta, G.A. (2024). Climate change impacts and adaptations of wine production. *Nature Reviews Earth and Environment*, *5*, 258–275. https://doi.org/10.1038/s43017-024-00521-5.

Longo, R., Carew, A., Sawyer, S., Kemp, B., & Kerslake, F. (2021). A review on the aroma composition of *Vitis vinifera* L. pinot noir wines: Origins and influencing factors. *Critical Reviews in Food Science and Nutrition*, *61*(10), 1589–1604. https://doi.org/10.1080/10408398.2020.1762535.

Medrano, H., Escalona, J.M., Bota, J., Gulías, J., & Flexas, J. (2002). Regulation of photosynthesis of C$_3$ plants in response to progressive drought: Stomatal conductance as a reference parameter. *Annals of Botany*, *89*, 895–905. https://doi.org/10.1093/aob/mcf079.

Noestheden, M., Noyovitz, B., Riordan-Short, S., Dennis, E.G., & Zandberg, W.F. (2018). Smoke from simulated forest fire alters secondary metabolites in *Vitis vinifera* L.

berries and wine. *Planta, 248*, 1537–1550. https://link.springer.com/article/10.1007/s00425-018-2994-7.

Palma-López, J., Sánchez-Rodríguez, A.R., del Campillo, M.C., León-Gutiérrez, J.M., & Ramírez-Pérez, P. (2024). Influence of soil properties on grape and must quality in the MontillaMoriles protected designation of origin (southern Spain). *Catena*, *241*, 108041. https://doi.org/10.1016/j.catena.2024.108041.

Paolini, M., Ziller, L., Bertoldi, D., Bontempo, L., Larcher, R., Nicolini, G., & Camin, F. (2016). δ^{15}N from soil to wine in bulk samples and proline. *Journal of Mass Spectrometry*, *51*, 668–674. https://doi.org/10.1002/jms.3824.

Raco, B., Dotsika, E., Poutoukis, D., Battaglini, R., & Chantzi, P. (2015). O-H-C isotope ratio determination in wine in order to be used as a fingerprint of its regional origin. *Food Chemistry*, *168*, 588–594. https://doi.org/10.1016/j.foodchem.2014.07.043.

Reynard, J.S., Zufferey, V., Nicol, G., & Murisier, F. (2011). Soil parameters impact the vine-fruit-wine continuum by altering vine nitrogen status. *Journal International des Sciences de la Vigne et du Vin*, *45*(4), 211–221. https://doi.org/10.20870/oeno-one.2011.45.4.1502.

Sánchez, R., Rodríguez-Nogales, J.M., Fernández-Fernández, E., Gonzalez, M.R., Medina-Trujillo, L., & Martín, P. (2022). Volatile composition and sensory properties of wines from vineyards affected by iron chlorosis. *Food Chemistry*, *369*, 130850. https://doi.org/10.1016/j.foodchem.2021.130850.

Santos, J.A., Fraga, H., Malheiro, A.C., Moutinho-Pereira, J., Dinis, L.T., Correia, C., et al. (2020). A review of the potential climate change impacts and adaptation options for European viticulture. *Applied Sciences-Basel*, *10*, 3092. https://doi.org/10.3390/app10093092.

Sherman, E., Coe, M., Grose, C., Martin, D., & Greenwood, D.R. (2020). Metabolomics approach to assess the relative contributions of the volatile and non-volatile composition to expert quality eatings of pinot noir wine quality. *Journal of Agricultural and Food Chemistry*, *68*(47), 13380–13396. https://doi.org/10.1021/acs.jafc.0c04095.

Spangenberg, J.E., Vogiatzaki, M., & Zufferey, V. (2017). Gas chromatography and isotope ratio mass spectrometry of pinot noir wine volatile compounds (δ^{13}C) and solid residues (δ^{13}C, δ^{15}N) for the reassessment of vineyard water-status. *Journal of Chromatography A*, *1517*, 142–155. https://doi.org/10.1016/j.chroma.2017.08.038.

Spangenberg, J.E., & Zufferey, V. (2018). Changes in soil water availability in vineyards can be traced by the carbon and nitrogen isotope composition of dried wines. *Science of the Total Environment*, *635*, 178–187. https://doi.org/10.1016/j.scitotenv.2018.04.078.

Spangenberg, J.E., & Zufferey, V. (2019). Carbon isotope composition of whole wine, wine solid residue, and wine ethanol, determined by EA/IRMS and GC/C/IRMS, can record the vine water status–a comparative reappraisal. *Analytical and Bioanalytical Chemistry*, *411*, 2031–2043. https://link.springer.com/article/10.1007/s00216-019-01625-4.

Spangenberg, J.E., & Zufferey, V. (2023). Soil management affects carbon and nitrogen concentrations and stable isotope ratios in vine products. *Science of the Total Environment*, *873*, 162410. doi.org/10.1016/j.scitotenv.2923.162410.

Tassoni, A., Tango, N., & Ferri, M. (2013). Comparison of biogenic amine and polyphenol profiles of grape berries and wines obtained following conventional, organic and biodynamic agricultural and oenological practices. *Food Chemistry*, *139*, 405–413. https://doi.org/10.1016/j.foodchem.2013.01.041.

Tonietto, J., & Carbonneau, A. (2004). A multicriteria climatic classification system for grape-growing regions worldwide. *Agricultural and Forest Meteorology*, *124*, 81–97. https://doi.org/10.1016/j.agrformet.2003.06.001.

de Torres, C., Diaz-Maroto, M.C., Hermosin-Gutierrez, I., & Perez-Coello, M.S. (2010). Effect of freeze-drying and oven-drying on volatiles and phenolics composition of grape skin. *Analytica Chimica Acta*, *660*, 177–182. https://doi.org/10.1016/j.aca.2009.10.005.

Ubeda, C., Hornedo-Ortega, R., Cerezo, A.B., Garcia-Parrilla, M.C., & Troncoso, A.M. (2020). Chemical hazards in grapes and wine, climate change and challenges to face. *Food Chemistry*, *314*, 126222. https://doi.org/10.1016/j.foodchem.2020.126222.

Verdenal, T., Spangenberg, J.E., Zufferey, V., Lorenzini, F., Spring, J.L., & Viret, O. (2015). Effect of fertilisation timing on the partitioning of foliar-applied nitrogen in Vitis vinifera cv. Chasselas: A N-15 labelling approach. *Australian Journal of Grape and Wine Research*, *21*, 110–117. https://doi.org/10.1111/ajgw.12116.

Wang, J., Gambetta, J.M., & Jeffery, D.M. (2016). Comprehensive study of volatile compounds in two Australian rosé wines: Aroma extract dilution analysis (AEDA) of extracts prepared using solvent-assisted flavor evaporation (SAFE) or headspace solid-phase extraction (HS-SPE). *Journal of Agricultural and Food Chemistry*, *64*, 3838–3848. https://pubs.acs.org/doi/10.1021/acs.jafc.6b01030.

Zufferey, V., Spring, J.L., Verdenal, T., Dienes, A., Belcher, S., Lorenzini, F., … Viret, O. (2017). Influence of water stress on plant hydraulics, gas exchange, berry composition and quality of pinot noir wines in Switzerland. *OENO one*, *51*, 37–57. https://doi.org/10.20870/oeno-one.2017.51.1.1314.